




PrEP Intervention in the Mitigation of HIV/AIDS Epidemics in China via a Data-Validated Age-Structured Model

Peng Wu¹ · Shohel Ahmed² · Xiunan Wang³ · Hao Wang² 

Received: 22 December 2022 / Accepted: 13 March 2023

© The Author(s), under exclusive licence to Society for Mathematical Biology 2023

Abstract

Antiretroviral-based pre-exposure prophylaxis (PrEP) treatment offers a new opportunity for protecting humans against HIV and disrupting current HIV prevention systems. However, implementing this preventive measure has been difficult due to its high cost. In this paper, we propose an age-structured model that incorporates infection ages, HAART (highly active antiretroviral therapy), and PrEP intervention. We investigate the qualitative behavior of the model and find a threshold parameter (the basic reproduction number) that determines the asymptotic stability of equilibria. We validate the model and estimate the parameters by confronting the actual HIV/AIDS data from 2004 to 2018 in China using MCMC (Markov Chain Monte Carlo) method. Furthermore, we investigate the PrEP intervention strategy by using incremental cost-effectiveness and average cost-effectiveness. Our work suggests that PrEP intervention based on the infection characteristics of different age groups can be an effective strategy to eradicate HIV/AIDS epidemics in China.

Keywords HIV/AIDS epidemics · Antiretroviral-based pre-exposure prophylaxis (PrEP) · Age structure · Antiretroviral therapy · Markov Chain Monte Carlo (MCMC)

1 Introduction

The HIV/AIDS epidemic has become a global pandemic and is one of the foremost public health problems in the world today. In China, the first domestic outbreak of HIV was detected in 1989 in an extremely remote rural area in Yunnan province. The

✉ Hao Wang
hao8@ualberta.ca

¹ School of Sciences, Hangzhou Dianzi University, Hangzhou 310018, People's Republic of China

² Department of Mathematical and Statistical Sciences, University of Alberta, Edmonton, AB T6G 2G1, Canada

³ Department of Mathematics, University of Tennessee at Chattanooga, Chattanooga, TN 37403, USA

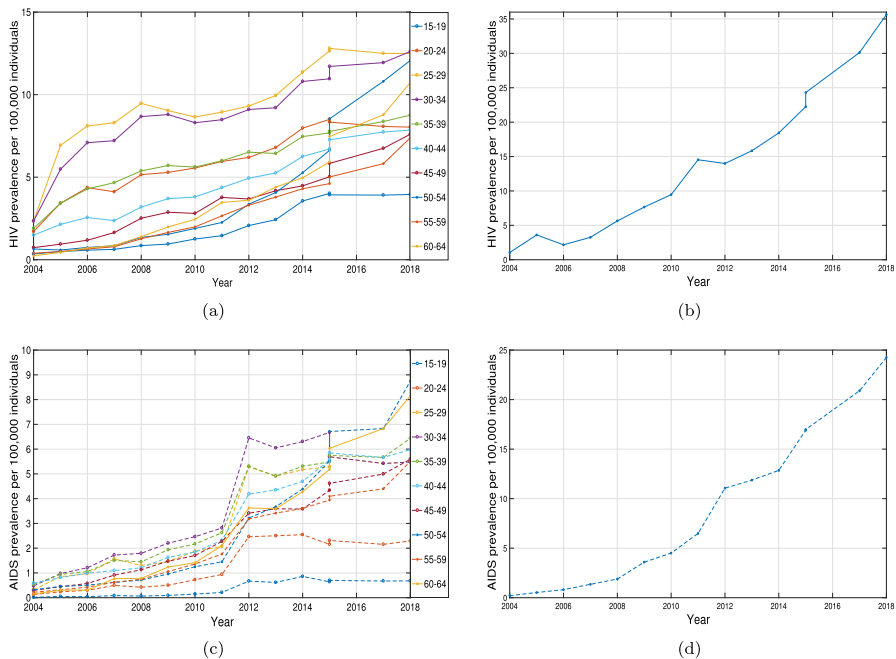


Fig. 1 **a** HIV prevalence per 100,000 individuals in 10 age groups from 15 to 64 years old. **b** HIV prevalence per 100,000 individuals in the 65+ age group; **c** AIDS prevalence per 100,000 individuals in 10 age groups from 15 to 64 years old. **d** AIDS prevalence per 100,000 individuals in the 65+ age group. Prevalence of the i -th age group = $\frac{\text{Number of new cases of the } i\text{-th age group}}{\text{The total population of the } i\text{-th age group}} \times 100,000$

total number of HIV notifications in China has steadily increased in recent years. The number of 146 reported cases in 1989 has grown to more than 1.25 million reported cases as we entered 2019 (Wu et al. 2020a). HIV infection is well known for its long incubation and infectious period, estimated at 8–10 years on average. The infectivity of HIV-infected people varies depending on the time since infection (infection age). For this reason, it is important to consider the infection-age structure when modeling HIV infection at the population level. In Fig. 1, we can see that the prevalence of HIV/AIDS continues to increase in different age groups, which motivates us to use mathematical models with age structure to analyze the prevalence of HIV in China.

Over the past 20 years, many epidemiology compartment models have been formulated to study the dynamics of HIV infection within the host and transmission among the population. Nelson et al. (2004) developed and analyzed an age-structured model of HIV-1 infection that allows for variations in the death rate of productively infected T cells and the production rate of viral particles as a function of the length of time a when T cell has been infected. Rong et al. (2007) presented an age-structured HIV-1 dynamics with the combination of antiretroviral therapy to study the influence of drug therapy on the within-host viral fitness and the possible development of drug-resistant strains. A structured novel Lyapunov function has been developed to investigate the global stability of the age-structured HIV infection model (Gang et al. 2012). Guo et al. (2021) established and analyzed a mathematical model that includes sequential

cell-free virus infection and cell-to-cell transmission. Wang et al. studied the global dynamics of an age-structured within-host HIV model with multiple target cells in Wang et al. (2017). Manoj and Abbas (2022) investigated the threshold dynamics of an age-structured model for HIV viral dynamics with latently infected T cells.

Due to the long infectious period of HIV epidemic, the age structure of a population has been regarded as a crucial factor for epidemiology modeling. Stavros and Chavez (1991) studied a general solution to the problem of mixing subpopulations and its application to the risk and age-structured epidemic models for the spread of AIDS. Afterward, some works investigated the threshold dynamics of the disease including the basic reproduction number derivation and the stability of steady states of the system. We refer readers to Martcheva and Crispino-O'Connell (2003), Webb (2008), Li et al. (2020), Qiu and Feng (2010), Chavez and Feng (1998), Feng et al. (2005), and the references therein. Another important research problem in age-structured infectious disease modeling is numerical implementation. Different from the constant-valued parameters of an ODE compartment model, an age-structured model contains some age-dependent parameters (such as mortality, infection rate, treatment rate, etc.), which brings great challenges to the numerical simulation of an age-structured model, especially how to combine model numerical simulation with actual epidemic data. In view of this, Hethcote (2000) first provided a method that converts an age-structured model into a demographic model and then uses actual data for numerical simulation. Angulo et al. (2007) investigated the application of an age-structured model with unbounded mortality to demography based on the data from 1990 to 2000 in the USA. Afterward, Angulo et al. presented a numerical method for nonlinear age-structured population models with finite maximum age in Angulo et al. (2010). Feng et al. (2020) studied the influence of demographically realistic mortality schedules on vaccination strategies in age-structured models. Based on Feng et al. (2020), Xue et al. (2022) constructed an evaluating strategy for tuberculosis to achieve the goals of WHO in China: a seasonal age-structured model study. Recently, Zhao et al. (2020) formulated a three-age-class ordinary differential equations HIV/AIDS model to investigate the transmission dynamics and optimal control strategy of HIV/AIDS in China. Since HIV transmission is highly sensitive in certain age groups, we would like to study HIV transmission in different age groups in detail.

The structure of this paper is organized as follows. In Sect. 2, we formulate the age-structured HIV/AIDS model with PrEP intervention for the transmission dynamics of HIV/AIDS. We obtain a non-dimensional form of the model in Sect. 3 and discuss the existence of the positive solution in Sect. 4. We derive the basic reproduction number and prove the stability of the disease-free steady state in Sect. 5. We show the existence and stability of the endemic steady state of the system in Sect. 6. We derive the demographic model corresponding to the age-structured model and conduct the numerical simulations in Sect. 7. In Sect. 8, we present the numerical simulations and PrEP intervention strategy. Finally, we close the paper with a discussion in Sect. 9.

2 Model Formulation

We formulate an age-structured epidemiological model to study HIV/AIDS transmission dynamics assuming the population is stratified by age due to the age-dependent force of infection. Moreover, we consider two treatment window periods for HIV diagnosis: high-efficiency antiretroviral therapy (HAART) and pre-exposure therapy (PrEP). The model divides the density of the total population $N(t, a)$ into six sub-compartments: susceptible individuals $S(t, a)$, HIV-infected individuals who are undiagnosed $L(t, a)$, HIV-infected individuals who have been diagnosed $I(t, a)$, HIV-infected individuals under HAART treatment $T(t, a)$, HIV-infected individuals with clinical symptoms (AIDS) $A(t, a)$ and susceptible individuals who take PrEP $E(t, a)$. We describe the disease dynamics using the following differential equations:

$$\left\{ \begin{array}{l} \frac{\partial S}{\partial a} + \frac{\partial S}{\partial t} = -\beta(t, a)S(t, a) - (\mu(a) + \psi(a))S(t, a) + \theta(a)E(t, a), \\ \frac{\partial L}{\partial a} + \frac{\partial L}{\partial t} = \beta(t, a)S(t, a) - \mu(a)L(t, a) - \phi(a)L(t, a), \\ \frac{\partial I}{\partial a} + \frac{\partial I}{\partial t} = \phi(a)L(t, a) - \gamma I(t, a) - \mu(a)I(t, a), \\ \frac{\partial T}{\partial a} + \frac{\partial T}{\partial t} = \omega(a)\gamma I(t, a) - \mu(a)T(t, a) - \alpha(a)T(t, a), \\ \frac{\partial A}{\partial a} + \frac{\partial A}{\partial t} = (1 - \omega(a))\gamma I(t, a) + \alpha(a)T(t, a) - (\mu(a) + d(a))A(t, a), \\ \frac{\partial E}{\partial a} + \frac{\partial E}{\partial t} = \psi(a)S(t, a) - \theta(a)E(t, a) - \mu(a)E(t, a), \end{array} \right. \quad (1)$$

with boundary and initial conditions:

$$\begin{aligned} S(t, 0) &= \Lambda, \quad L(t, 0) = 0, \quad I(t, 0) = 0, \quad T(t, 0) = 0, \\ A(t, 0) &= 0, \quad E(t, 0) = 0, \\ S(0, a) &= S_0(a), \quad L(0, a) = L_0(a), \quad I(0, a) = I_0(a), \quad T(0, a) = T_0(a), \\ A(0, a) &= A_0(a), \quad E(0, a) = E_0(a), \end{aligned}$$

where

$$\begin{aligned} \beta(t, a) &= \int_0^{a_+} \lambda(a, a') \frac{(\eta_L L(a', t) + I(a', t) + \eta_T T(a', t) + \eta_A A(a', t))}{N(a', t)} da', \\ N(t, a) &= S(t, a) + L(t, a) + I(t, a) + T(t, a) + A(t, a) + E(t, a), \\ \lambda(a, a') &= B(a)\bar{\beta}(a'), \end{aligned}$$

and $a_+ > 0$ is the maximum age of an individual.

The details of the variables and parameters are given in Table 1.

Table 1 Parameters and numerical values

Parameters and variables	Description
$S(t, a)$	Susceptible individuals of age a at time t
$L(t, a)$	HIV-infected individuals who are undiagnosed of age a at time t
$I(t, a)$	HIV-infected individuals who have been diagnosed of age a at time t
$T(t, a)$	HIV-infected individuals under HAART treatment of age a at time t
$A(t, a)$	HIV-infected individuals with clinical symptoms of age a at time t
$E(t, a)$	Susceptible individuals of age a who take PrEP at time t
$\lambda(a, a')$	Probability that an infective individual of age a' will contact and successfully infect a susceptible individual of age a
$B(a)$	The effective contact rate of age a
$\beta(a')$	The infection rate of age a'
$\mu(a)$	Age-dependent mortality rate
$\psi(a)$	The proportion of individuals of age a that take PrEP
$\theta(a)$	The proportion of the individuals of age a that stop taking safety measures and become susceptible again
$\phi(a)$	The rate of $L(a, t)$ moving to $I(a, t)$
$\omega(a)$	The proportion of HIV-infected individuals who take HAART treatment
γ	The rate moving out of the diagnosed compartment to get HAART treatment or develop clinical symptoms
$\alpha(a)$	The rate of $T(a, t)$ moving to $A(a, t)$
$d(a)$	Age-dependent HIV-related mortality rate

3 Preliminary Work

In this section, we will nondimensionalize model (1) for further study. The total population $N(a, t)$ satisfies the following equations

$$\frac{\partial N}{\partial a} + \frac{\partial N}{\partial t} = -\mu(a)N(a, t) - d(a)A(a, t), \quad (2)$$

with boundary and initial conditions

$$\begin{aligned} N(0, t) &= S(0, t) + L(0, t) + I(0, t) + T(0, t) + A(0, t) + E(0, t) = \Lambda, \\ N(a, 0) &= N_0(a) = S_0(a) + L_0(a) + I_0(a) + T_0(a) + A_0(a) + E_0(a). \end{aligned}$$

Let

$$\begin{aligned} x(t, a) &= \frac{S(t, a)}{N(t, a)}, \quad y(t, a) = \frac{L(t, a)}{N(t, a)}, \quad z(t, a) = \frac{I(t, a)}{N(t, a)}, \\ u(t, a) &= \frac{T(t, a)}{N(t, a)}, \quad v(t, a) = \frac{A(t, a)}{N(t, a)}, \quad w(t, a) = \frac{E(t, a)}{N(t, a)}, \end{aligned}$$

that gives

$$\begin{aligned} \frac{\partial S}{\partial a} + \frac{\partial S}{\partial t} &= \left(\frac{\partial x}{\partial a} + \frac{\partial x}{\partial t} \right) N(a, t) + \left(\frac{\partial N}{\partial a} + \frac{\partial N}{\partial t} \right) x(a, t), \\ \frac{\partial x}{\partial a} + \frac{\partial x}{\partial t} &= -(\psi(a) - d(a)v(a, t))x(a, t) - \delta(a, t)x(a, t) + \theta(a)w(a, t). \end{aligned}$$

Similarly, apply this transformation to other variables of model (1); then, system (1) can be rewritten as the following nondimensional form:

$$\left\{ \begin{aligned} \frac{\partial x}{\partial a} + \frac{\partial x}{\partial t} &= -\delta(a, t)x(a, t) - (\psi(a) - d(a)v(a, t))x(a, t) + \theta(a)w(a, t), \\ \frac{\partial y}{\partial a} + \frac{\partial y}{\partial t} &= \delta(a, t)x(a, t) - (\phi(a) - d(a)v(a, t))y(a, t), \\ \frac{\partial z}{\partial a} + \frac{\partial z}{\partial t} &= \phi(a)y(a, t) - (\gamma - d(a)v(a, t))z(a, t), \\ \frac{\partial u}{\partial a} + \frac{\partial u}{\partial t} &= \omega(a)\gamma z(a, t) - (\alpha(a) - d(a)v(a, t))u(a, t), \\ \frac{\partial v}{\partial a} + \frac{\partial v}{\partial t} &= (1 - \omega(a))\gamma z(a, t) + \alpha(a)u(a, t) - d(a)(1 - v(a, t))v(a, t), \\ \frac{\partial w}{\partial a} + \frac{\partial w}{\partial t} &= \psi(a)x(a, t) - (\theta(a) - d(a)v(a, t))w(a, t), \end{aligned} \right. \quad (3)$$

where $\delta(a, t) = \int_0^{a+} \lambda(a, a') (\eta_L y(a', t) + z(a', t) + \eta_T u(a', t) + \eta_A v(a', t)) da'$.

Corresponding initial values and boundary conditions for system (3) are

$$\begin{aligned} x(0, t) &= 1, \quad y(0, t) = 0, \quad z(0, t) = 0, \quad u(0, t) = 0, \\ v(0, t) &= 0, \quad w(0, t) = 0, \\ x(a, 0) &= x_0(a), \quad y(a, 0) = y_0(a), \quad z(a, 0) = z_0(a), \\ u(a, 0) &= u_0(a), \quad v(a, 0) = v_0(a), \quad w(a, 0) = w_0(a). \end{aligned}$$

4 Qualitative Study of the Model

In order to retain the biological validity of the model, in this section, we will show the solutions to system (3) exist and they are positive for all values of the time.

Consider the Banach space

$$X = L^1(0, a_+) \times L^1(0, a_+) \times L^1(0, a_+) \times L^1(0, a_+) \times L^1(0, a_+) \times L^1(0, a_+),$$

endowed with the norm

$$\|\Phi\| = \sum_{i=1}^6 \|\Phi_i\|, \quad \Phi(a) = (\Phi_1(a), \Phi_2(a), \Phi_3(a), \Phi_4(a), \Phi_5(a), \Phi_6(a))^T \in X.$$

Here $\|\cdot\|$ is the norm of space $L^1(0, a_+)$. Denote

$$\Omega := \{(x, y, z, u, v, w) \in X_+ | 0 \leq x + y + z + u + v + w \leq 1\}$$

as the state space of system (3), where $X_+ = L^1_+(0, a_+) \times L^1_+(0, a_+) \times L^1_+(0, a_+) \times L^1_+(0, a_+) \times L^1_+(0, a_+) \times L^1_+(0, a_+)$, and the positive cone of $L^1(0, a_+)$ is $L^1_+(0, a_+)$. The linear operator \mathcal{A} is given by

$$(\mathcal{A}\Phi)(a) = \vec{\mathcal{A}},$$

where

$$\vec{\mathcal{A}} = \begin{pmatrix} -\frac{dx}{da} - \psi(a) & 0 & 0 & 0 & 0 & \theta(a) \\ 0 & -\frac{dy}{da} - \phi(a) & 0 & 0 & 0 & 0 \\ 0 & \phi(a) & -\frac{dz}{da} - r & 0 & 0 & 0 \\ 0 & 0 & \omega(a)r & -\frac{du}{da} - \alpha(a) & 0 & 0 \\ 0 & 0 & (1 - \omega(a))r & \alpha(a) & -\frac{dv}{da} - d(a) & 0 \\ \psi(a) & 0 & 0 & 0 & 0 & -\frac{dw}{da} - \theta(a) \end{pmatrix}, \tag{4}$$

and the domain $D(\mathcal{A})$ is given as

$$D(\mathcal{A}) = \{\Phi \in X | \Phi_i \in BC[0, a_+), \Phi(0) = (1, 0, 0, 0, 0, 0)\},$$

where $BC[0, a_+)$ denotes the set of absolutely continuous functions on $[0, a_+)$. The nonlinear operator $\mathcal{F} : X \rightarrow X$ is given by

$$(\mathcal{F}\Phi)(a) = \bar{\mathcal{F}},$$

where

$$\bar{\mathcal{F}} = \begin{pmatrix} d(a)\Phi_1\Phi_5 - (\eta_L(M\Phi_2)(a) + (M\Phi_3)(a) + \eta_T(M\Phi_4)(a) + \eta_A(M\Phi_5)(a))\Phi_1 \\ (\eta_L(M\Phi_2)(a) + (M\Phi_3)(a) + \eta_T(M\Phi_4)(a) + \eta_A(M\Phi_5)(a))\Phi_1 \\ d(a)\Phi_3\Phi_5 \\ d(a)\Phi_4\Phi_5 \\ d(a)(\Phi_5)^2 \\ d(a)\Phi_6\Phi_5 \end{pmatrix}, \tag{5}$$

where M is a bounded linear operator on $L^1(0, a_+)$ given by

$$(Mf)(a) = \int_0^{a_+} \lambda(a, a') f(a') da'.$$

Denote $m(t) = (x(\cdot, t), y(\cdot, t), z(\cdot, t), u(\cdot, t), v(\cdot, t), w(\cdot, t))$, then system (3) can be rewritten as follows

$$\frac{dm(t)}{dt} = \mathcal{A}m(t) + \mathcal{F}(m(t)), \quad m(0) = m_0 \in X, \tag{6}$$

where $m_0 = (x_0(a), y_0(a), z_0(a), u_0(a), v_0(a), w_0(a))^T$.

For \mathcal{A} and \mathcal{F} , using results from Webb (2008), we have the following conclusions:

Lemma 1 *The space Ω is positively invariant associated with the semiflow defined by $e^{\mathcal{A}t}$, where $e^{\mathcal{A}t}$ is a C_0 -semigroup generated by the linear operator \mathcal{A} .*

Lemma 2 *The operator \mathcal{F} is continuously Frechet differentiable on X .*

Theorem 4.1 *There exists a maximal existence interval $[0, t_0)$ and a mild solution $m(t, m_0) \in X_+$, $t \in [0, t_0)$ for system (6) such that*

$$m(t) = e^{\mathcal{A}t} m_0 + \int_0^t e^{\mathcal{A}(t-\tau)} \mathcal{F}(m(\tau)) d\tau \text{ for each } m_0 \in X_+.$$

Thus, the solutions to system (3) exist for all $t \in [0, t_0]$.

5 Basic Reproduction Number and Stability of the Disease-Free Equilibrium

The positive steady state $(x(a), y(a), z(a), u(a), v(a), w(a))$ of system (3) satisfies the following equations

$$\left\{ \begin{aligned} \frac{dx}{da} &= -\delta(a)x(a) - (\psi(a) - d(a)v(a))x(a) + \theta(a)w(a), \\ \frac{dy}{da} &= \delta(a)x(a) - (\phi(a) - d(a)v(a))y(a), \\ \frac{dz}{da} &= \phi(a)y(a) - (r - d(a)v(a))z(a), \\ \frac{du}{da} &= \omega(a)rz(a) - (\alpha(a) - d(a)v(a))u(a), \\ \frac{dv}{da} &= (1 - \omega(a))rz(a) + \alpha(a)u(a) - d(a)(1 - v(a))v(a), \\ \frac{dw}{da} &= \psi(a)x(a) - (\theta(a) - d(a)v(a))w(a), \end{aligned} \right. \tag{7}$$

where $\delta(a) = \int_0^{a+} \lambda(a') (\eta_L y(a') + z(a') + \eta_T u(a') + \eta_A v(a')) da'$ and initial conditions are

$$x(0) = 1, y(0) = 0, z(0) = 0, u(0) = 0, v(0) = 0, q(0) = 0.$$

Denote the disease-free equilibrium as $E_0 = (x^0(a), y^0(a), z^0(a), u^0(a), v^0(a), w^0(a))$. Because $y^0(a) = z^0(a) = u^0(a) = v^0(a) = 0$ and $w^0(a) = 1 - x^0(a)$, which implies $\delta(a) = 0$, from the first equation of system (7) we have

$$\begin{aligned} x^0(a) &= \exp \left\{ - \int_0^a (\psi(\xi) + \theta(\xi)) d\xi \right\} \\ &+ \int_0^a \theta(\eta) \exp \left\{ - \int_\eta^a (\psi(\xi) + \theta(\xi)) d\xi \right\} d\eta. \end{aligned} \tag{8}$$

To study the stability of the disease-free equilibrium E_0 , we denote the perturbations by $\tilde{x}(a, t), \tilde{y}(a, t), \tilde{z}(a, t), \tilde{u}(a, t), \tilde{v}(a, t), \tilde{w}(a, t)$, respectively. Then, we have

$$\left\{ \begin{aligned} \frac{\partial \tilde{x}}{\partial a} + \frac{\partial \tilde{x}}{\partial t} &= -(d(a)\tilde{v}(a, t) + \tilde{\delta}(a, t)) x_a^0 - \psi(a)\tilde{v}(a, t)x(a, t) + \theta(a)\tilde{w}(a, t), \\ \frac{\partial \tilde{y}}{\partial a} + \frac{\partial \tilde{y}}{\partial t} &= \tilde{\delta}(a, t)x^0(a) - \phi(a)\tilde{y}(a, t), \\ \frac{\partial \tilde{z}}{\partial a} + \frac{\partial \tilde{z}}{\partial t} &= \phi(a)\tilde{y}(a, t) - r\tilde{z}(a, t), \\ \frac{\partial \tilde{u}}{\partial a} + \frac{\partial \tilde{u}}{\partial t} &= \omega(a)r\tilde{z}(a, t) - \alpha(a)\tilde{u}(a, t), \\ \frac{\partial \tilde{v}}{\partial a} + \frac{\partial \tilde{v}}{\partial t} &= (1 - \omega(a))r\tilde{z}(a, t) + \alpha(a)\tilde{u}(a, t) - d(a)\tilde{v}(a, t), \\ \frac{\partial \tilde{w}}{\partial a} + \frac{\partial \tilde{w}}{\partial t} &= \psi(a)\tilde{x}(a, t) - \theta(a)\tilde{w}(a, t) + d(a)\tilde{v}(a, t)w^0(a), \end{aligned} \right. \tag{9}$$

where $\tilde{\delta}(a, t) = B(a) \int_0^{a+} \tilde{\beta}(a') (\eta_L \tilde{y} + \tilde{z} + \eta_T \tilde{u} + \eta_A \tilde{v}) (a', t) da'$, with boundary conditions:

$$\tilde{x}(0, t) = 1, \tilde{y}(0, t) = 0, \tilde{z}(0, t) = 0, \tilde{u}(0, t) = 0, \tilde{v}(0, t) = 0, \tilde{w}(0, t) = 0.$$

We set

$$\begin{aligned} \tilde{x}(a, t) &= \tilde{x}(a)e^{\sigma t}, \tilde{y}(a, t) = \tilde{y}(a)e^{\sigma t}, \tilde{z}(a, t) = \tilde{z}(a)e^{\sigma t}, \\ \tilde{u}(a, t) &= \tilde{u}(a)e^{\sigma t}, \tilde{v}(a, t) = \tilde{v}(a)e^{\sigma t}, \tilde{w}(a, t) = \tilde{w}(a)e^{\sigma t}, \end{aligned}$$

where $\tilde{x}(a), \tilde{y}(a), \tilde{z}(a), \tilde{u}(a), \tilde{v}(a), \tilde{w}(a)$, and the growth exponent σ satisfy the following equations:

$$\left\{ \begin{aligned} \frac{d\tilde{x}}{da} &= -\sigma \tilde{x}(a) - \left(d(a)\tilde{v}(a) + \tilde{\delta}(a) \right) x_a^0 - \psi(a)\tilde{v}(a)x(a) + \theta(a)\tilde{w}(a), \\ \frac{d\tilde{y}}{da} &= -\sigma \tilde{y}(a) + \tilde{\delta}(a)x^0(a) - \phi(a)\tilde{y}(a), \\ \frac{d\tilde{z}}{da} &= -\sigma \tilde{z}(a) + \phi(a)\tilde{y}(a) - r\tilde{z}(a), \\ \frac{d\tilde{u}}{da} &= -\sigma \tilde{u}(a) + \omega(a)r\tilde{z}(a) - \alpha(a)\tilde{u}(a), \\ \frac{d\tilde{v}}{da} &= -\sigma \tilde{v}(a) + (1 - \omega(a))r\tilde{z}(a) + \alpha(a)\tilde{u}(a) - d(a)\tilde{v}(a), \\ \frac{d\tilde{w}}{da} &= -\sigma \tilde{w}(a) + \psi(a)\tilde{x}(a) - \theta(a)\tilde{w}(a) + d(a)\tilde{v}(a)w^0(a), \end{aligned} \right. \tag{10}$$

where $\tilde{\lambda}(a) = B(a) \int_0^{a+} \tilde{\beta}(a) (\eta_L \tilde{y} + \tilde{z} + \eta_T \tilde{u} + \eta_A \tilde{v}) (a) da$, with boundary conditions:

$$\tilde{x}(0) = 0, \tilde{y}(0) = 0, \tilde{z}(0) = 0, \tilde{u}(0) = 0, \tilde{v}(0) = 0, \tilde{w}(0) = 0.$$

Let $\Pi = \int_0^{a+} \tilde{\beta}(a) (\eta_L \tilde{y} + \tilde{z} + \eta_T \tilde{u} + \eta_A \tilde{v}) (a) da$, then $\tilde{\lambda}(a) = B(a)\Pi$. From the second equation of system (10), we obtain

$$\tilde{y}' + (\sigma + \phi(a)) \tilde{y} = B(a)\Pi x^0(a),$$

then

$$\tilde{y}(a) = \Pi \int_0^a B(\eta)x^0(\eta) \exp \left\{ - \int_\eta^a (\sigma + \phi(\xi))d\xi \right\} d\eta.$$

Next, we obtain the expression of $\tilde{z}(a)$ from the third equation of system (10) as

$$\tilde{z}(a) = \int_0^a \phi(\eta)\tilde{y}(\eta)e^{-(\sigma+r)(a-\eta)} d\eta.$$

Similarly, we have

$$\begin{aligned} \tilde{u}(a) &= \int_0^a \omega(\eta)r\tilde{z}(\eta) \exp \left\{ - \int_{\eta}^a (\alpha(\xi) + \sigma)d\xi \right\} d\eta, \\ \tilde{v}(a) &= \int_0^a [(1 - \omega(\eta))r\tilde{z}(\eta) + \alpha(\eta)\tilde{u}(\eta)] \exp \left\{ - \int_{\eta}^a (d(\xi) + \sigma)d\xi \right\} d\eta. \end{aligned}$$

Define $\int_0^a B(\eta)x^0(\eta) \exp \left\{ - \int_{\eta}^a (\sigma + \phi(\xi))d\xi \right\} d\eta = \Gamma(a)$, then $\tilde{y}(a) = \Pi\Gamma(a)$. The expression of $\tilde{z}(a)$ and $\tilde{u}(a)$ can be rewritten as

$$\begin{aligned} \tilde{z}(a) &= \Pi \int_0^a \phi(\eta)\Gamma(\eta)e^{-(\sigma+r)(a-\eta)}d\eta = \Pi\Psi(a), \\ \tilde{u}(a) &= \Pi r \int_0^a \omega(\eta)\Psi(\eta) \exp \left\{ - \int_{\eta}^a (\alpha(\xi) + \sigma) \right\} d\eta = r\Pi Q(a), \end{aligned} \tag{11}$$

where $\Psi(a) = \int_0^a \phi(\eta)\Gamma(\eta)e^{-(\sigma+r)(a-\eta)}d\eta$, $Q(a) = \int_0^a \omega(\eta)\Psi(\eta) \exp \left\{ - \int_{\eta}^a (\alpha(\xi) + \sigma) \right\} d\eta$. Substituting (11) in the expression of $\tilde{v}(a)$ yields

$$\tilde{v}(a) = r\Pi \int_0^a [(1 - \omega(\eta))\Psi(\eta) + \alpha(\eta)Q(\eta)] \exp \left\{ - \int_{\eta}^a (d(\xi) + \sigma)d\xi \right\} d\eta.$$

Consider the expression of Π , substituting the \tilde{y} , \tilde{z} , \tilde{u} , \tilde{v} into Π , then we obtain that

$$\begin{aligned} 1 &= \int_0^{a+} \bar{\beta}(a)\Psi(a)da + r\eta_L \int_0^{a+} \bar{\beta}(a)\Gamma(a)da + r\eta_T \int_0^{a+} \bar{\beta}(a)Q(a)da \\ &+ r\eta_A \int_0^{a+} \bar{\beta}(a) \int_0^a \left((1 - \omega(\eta))\Psi(\eta) + \alpha(\eta)Q(\eta) \right) \\ &\exp \left\{ - \int_{\eta}^a (\sigma + d(\xi))d\xi \right\} d\eta. \end{aligned} \tag{12}$$

Denote the right hand side of (12) by $G(\sigma)$, then the basic reproduction number $\mathcal{R}(\psi, \theta) = G(0)$ or can be explicitly written

$$\begin{aligned} \mathcal{R}(\psi, \theta) &= \int_0^{a+} \bar{\beta}(a)\tilde{\Psi}(a)da + r\eta_L \int_0^{a+} \bar{\beta}(a)\tilde{\Gamma}(a)da + r\eta_T \int_0^{a+} \bar{\beta}(a)\tilde{Q}(a)da \\ &+ r\eta_A \int_0^{a+} \bar{\beta}(a) \int_0^a \left((1 - \omega(\eta))\tilde{\Psi}(\eta) + \alpha(\eta)\tilde{Q}(\eta) \right) \\ &\exp \left\{ - \int_{\eta}^a d(\xi)d\xi \right\} d\eta, \end{aligned} \tag{13}$$

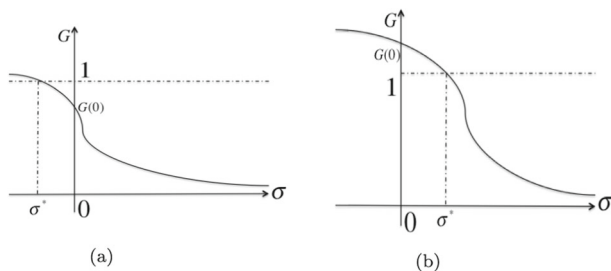


Fig. 2 **a** Function image of $G(\sigma)$ when $G(0) < 1$, **b** the function image of $G(\sigma)$ when $G(0) > 1$

where

$$\begin{aligned} \tilde{\Gamma}(a) &= \int_0^a B(\eta)x^0(\eta) \exp \left\{ - \int_\eta^a \phi(\xi)d\xi \right\} d\eta, \\ \tilde{\Psi}(a) &= \int_0^a \phi(\eta)\tilde{\Gamma}(\eta)e^{-r(a-\eta)} d\eta, \\ \tilde{Q}(a) &= \int_0^a \omega(\eta)\tilde{\Psi}(\eta) \exp \left\{ - \int_\eta^a \alpha(\xi) \right\} d\eta. \end{aligned}$$

Now, we investigate the local stability of the disease-free equilibrium.

Theorem 5.1 *There exists a maximal existence interval $[0, t_0)$ and a mild solution $m(t, m_0) \in X_+$, $t \in [0, t_0)$ for system (6) such that the disease-free equilibrium E_0 is stable if $\mathcal{R}(\psi, \theta) < 1$ and unstable if $\mathcal{R}(\psi, \theta) > 1$.*

Proof The function $G(\sigma)$ (the right hand side of (12)) is a decreasing and continuous function of σ which approaches ∞ as $\sigma \rightarrow -\infty$ and zero when $\sigma \rightarrow \infty$. Therefore, the characteristic equation (12) has a unique real solution σ^* . If $G(0) < 1$, i.e., $\mathcal{R}(\psi, \theta) < 1$, then the unique real eigenvalue is negative (see Fig. 2a). If $G(0) > 1$, $\mathcal{R}(\psi, \theta) > 1$, then the unique real solution of (12) is positive and E_0 is unstable (see Fig. 2b).

Furthermore, equation (12) has complex roots. Let $\sigma = a + bi$, since $\text{Re}(e^\sigma) \leq e^{Re\sigma}$, from (12) we know that $ReG(\sigma) = 1$, $\text{Im}G(\sigma) = 0$, and $1 \leq G(Re\sigma)$. It follows that $Re\sigma \leq \sigma^*$, since $G(\sigma)$ is a decreasing function of σ , that is, all complex solutions of (12) have real parts smaller than σ^* (< 0). Thus, E_0 is stable if $\mathcal{R}(\psi, \theta) < 1$. The proof completes. □

In order to understand the influence of PrEP, we compare the basic reproduction number $\mathcal{R}(\psi, \theta)$ with \mathcal{R}_0 , which is the basic reproduction number without PrEP treatment. We obtain the following expression for \mathcal{R}_0 without w equation by setting $\psi(a) = \theta(a) = 0$:

$$\begin{aligned}
 \mathcal{R}_0 &= \int_0^{a^+} \bar{\beta}(a)\widehat{\Psi}(a)da + r\eta_L \int_0^{a^+} \bar{\beta}(a)\widehat{\Gamma}(a)da + r\eta_T \int_0^{a^+} \bar{\beta}(a)\widehat{Q}(a)da \\
 &\quad + r\eta_A \int_0^{a^+} \bar{\beta}(a) \int_0^a \left((1 - \omega(\eta))\widehat{\Psi}(\eta) + \alpha(\eta)\widehat{Q}(\eta) \right) \\
 &\quad \exp \left\{ - \int_\eta^a d(\xi)d\xi \right\} d\eta, \\
 \widehat{\Gamma}(a) &= \int_0^a B(\eta) \exp \left\{ - \int_\eta^a \phi(\xi)d\xi \right\} d\eta, \quad \widehat{\Psi}(a) = \int_0^a \phi(\eta)\widehat{\Gamma}(\eta)e^{-r(a-\eta)}d\eta, \\
 \widehat{Q}(a) &= \int_0^a \omega(\eta)\widehat{\Psi}(\eta) \exp \left\{ - \int_\eta^a \alpha(\xi) \right\} d\eta.
 \end{aligned}
 \tag{14}$$

By equation (8), for all $a > 0$, $x^0(a) < 1$ except that $x^0(a) = 1$ when $\psi(a) = \theta(a) = 0$, which implies $\widehat{\Gamma}(a) > \widetilde{\Gamma}(a)$. Hence, $\mathcal{R}(\psi, \theta) < \mathcal{R}_0$ ($\mathcal{R}(\psi, \theta)$ is an increasing function with respect to $\widetilde{\Gamma}(a)$). When the reproductive number is greater than one in the absence of PrEP treatment, i.e., $\mathcal{R}_0 = R(0, 0) > 1$, treatment programs can be used to reduce the reproductive number $\mathcal{R}(\psi, \theta)$ to values below one and thereby can be helpful in controlling or eliminating the disease.

6 Study of the Endemic Equilibrium

In this section, we investigate the existence and stability of the endemic steady-state $E^* = (x^*(a), y^*(a), z^*(a), u^*(a), v^*(a), w^*(a))$.

Theorem 6.1 *If $\mathcal{R}(\psi, \theta) > 1$ and $d(a)=0$, then system (3) has a unique disease-endemic steady state E^* .*

Proof We denote $\delta^*(a) = B(a) \int_0^{a^+} \bar{\beta}(a) \left(\eta_L y^*(a) + z^*(a) + \eta_T u^*(a) + \eta_A v^*(a) \right) da = \Pi^* B(a)$. The coordinates of E^* satisfy the following equations:

$$\left\{ \begin{aligned}
 x^*(a) &= \int_0^a \theta(\eta)w^*(\eta) \exp \left\{ - \int_\eta^a \left(\psi(\xi) + \Pi^* B(\xi) \right) d\xi \right\} d\eta \\
 &\quad + \exp \left\{ - \int_0^a \left(\psi(\xi) + \Pi^* B(\xi) \right) d\xi \right\}, \\
 y^*(a) &= \int_0^a x^*(\eta)B(\eta)\Pi^* \exp \left\{ - \int_\eta^a \phi(\xi)d\xi \right\} d\eta, \\
 z^*(a) &= \int_0^a \phi(\eta)y^*(\eta) \exp \left\{ - \int_\eta^a r d\xi \right\} d\eta, \\
 u^*(a) &= \int_0^a \omega(\eta)r z^*(\eta) \exp \left\{ - \int_\eta^a \alpha(\xi)d\xi \right\} d\eta, \\
 v^*(a) &= \int_0^a \left((1 - \omega(\eta))r z^*(\eta) + \alpha(\eta)u^*(\eta) \right) d\eta, \\
 w^*(a) &= \int_0^a \psi(\eta)x^*(\eta) \exp \left\{ - \int_\eta^a \theta(\xi)d\xi \right\} d\eta,
 \end{aligned} \right.
 \tag{15}$$

where $\Pi^* = \int_0^{a+} \bar{\beta}(a) \left(\eta_L y^*(a) + z^*(a) + \eta_T u^*(a) + \eta_A v^*(a) \right) da$. Substituting $w^*(a)$ into $x^*(a)$, we obtain

$$\begin{aligned} x^*(a) &= \int_0^a \theta(\eta) \left(\int_0^\eta \psi(\xi) x^*(\xi) \exp \left\{ - \int_\xi^\eta \theta(\tau) d\tau \right\} d\xi \right) \\ &\quad \exp \left\{ - \int_\eta^a \left(\psi(\xi) + \Pi^* B(\xi) \right) d\xi \right\} d\eta \\ &\quad + \exp \left\{ - \int_0^a \left(\psi(\xi) + \Pi^* B(\xi) \right) d\xi \right\}. \end{aligned}$$

Exchanging the order of multiple integrals, we obtain that

$$x^*(a) = P_1(a) + \int_0^a P_2(a, \eta, \Pi^*) d\eta,$$

where

$$P_1(a) = \exp \left\{ - \int_0^a \left(\psi(\eta) + \Pi^* B(\eta) \right) d\eta \right\},$$

$$P_2(a, \eta, \Pi^*) = \psi(\eta) \int_\eta^a \theta(\xi) \exp \left\{ - \int_\xi^a \left(\psi(\tau) + \Pi^* B(\tau) \right) d\tau - \int_\eta^\xi \theta(\tau) d\tau \right\} d\xi.$$

Then, there is a unique solution $x^*(a, \Pi^*)$ which depends continuously on Π^* for every Π^* . Substituting $y^*(a)$ into $z^*(a)$ gives

$$\begin{aligned} z^*(a) &= \int_0^a \phi(\eta) y^*(\eta) e^{-r(a-\eta)} d\eta \\ &= \Pi^* \int_0^a \int_0^\eta \phi(\eta) x^*(\xi) B(\xi) \exp \left\{ - \int_\xi^a \phi(\tau) d\tau \right\} e^{-r(a-\eta)} d\xi d\eta. \end{aligned}$$

Thus, the expression of $u^*(a)$ is given by

$$\begin{aligned} u^*(a) &= r \Pi^* \int_0^a \int_0^\eta \int_0^\zeta \omega(\eta) \exp \left\{ - \int_\eta^a \alpha(\xi) d\xi \right\} \phi(\zeta) x^*(g) B(g) \\ &\quad \exp \left\{ - \int_g^a \phi(\xi) d\xi \right\} e^{-r(a-g)} dg d\zeta d\eta. \end{aligned}$$

With $u^*(a)$, $z^*(a)$, we have

$$\begin{aligned}
 v^*(a) = & r\Pi^* \int_0^a \left\{ (1 - \omega(\eta)) \int_0^\eta \int_0^\xi \phi(\xi)x^*(\zeta)B(\zeta) \right. \\
 & \exp \left\{ - \int_\zeta^a \phi(\tau)d\tau \right\} e^{-r(a-\zeta)} d\zeta d\xi \\
 & + \alpha(\eta) \int_0^\eta \int_0^\xi \int_0^\rho \omega(\xi) \\
 & \exp \left\{ - \int_\xi^a \alpha(\tau)d\tau \right\} x^*(g)B(g) \\
 & \left. \exp \left\{ - \int_g^a \phi(\tau)d\tau \right\} e^{-r(a-g)} dg d\rho d\xi \right\} d\eta.
 \end{aligned}$$

Substituting the expressions of $y^*(a)$, $z^*(a)$, $u^*(a)$, $v^*(a)$ into Π^* and canceling Π^* , we get

$$\begin{aligned}
 1 = & \int_0^{a+} \bar{\beta}(a)\eta_L \int_0^a x^*(\eta)B(\eta) \\
 & \exp \left\{ - \int_\eta^a \phi(\xi)d\xi \right\} d\eta da \\
 & + \int_0^{a+} \bar{\eta} \int_0^a \int_0^\eta \phi(\eta)x^*(\xi)B(\xi) \\
 & \exp \left\{ - \int_\xi^a \phi(\tau)d\tau \right\} e^{-r(a-\xi)} d\xi d\eta da \\
 & + \int_0^{a+} r\eta_T \bar{\beta}(a) \int_0^a \int_0^\eta \int_0^\zeta \omega(\eta) \exp \left\{ - \int_\eta^a \alpha(\xi)d\xi \right\} \phi(\zeta)x^*(g)B(g) \\
 & \exp \left\{ - \int_g^a \phi(\tau)d\tau \right\} e^{-r(a-g)} dg d\zeta d\eta da \tag{16} \\
 & + \eta_A \int_0^{a+} \bar{\beta}(a) \left\{ r \int_0^a \left\{ (1 - \omega(\eta)) \int_0^\eta \int_0^\xi \phi(\xi)x^*(\zeta)B(\zeta) \right. \right. \\
 & \exp \left\{ - \int_\zeta^a \phi(\tau)d\tau \right\} e^{-r(a-\zeta)} d\zeta d\xi \\
 & + \alpha(\eta) \int_0^\eta \int_0^\xi \int_0^\rho \omega(\xi) \exp \left\{ - \int_\xi^a \alpha(\tau)d\tau \right\} x^*(g)B(g) \\
 & \left. \left. \exp \left\{ - \int_g^a \phi(\tau)d\tau \right\} e^{-r(a-g)} dg d\rho d\xi \right\} d\eta \right\} da
 \end{aligned}$$

Denote the right-hand side of (16) by $\mathcal{H}(\Pi^*)$, then $\mathcal{H}(\Pi^*)$ is a continuous decreasing function of Π^* . Furthermore, $x^*(a, 0)$ is x^0 , which is the disease-free equilibrium. Therefore, $\mathcal{H}(0) = \mathcal{R}(\psi, \theta)$, that is, $\mathcal{R}(\psi, \theta) > 1$ implies $\mathcal{H}(0) > 1$. On the other

hand, based on $\Pi^* > 0$ and its expression we have

$$1 = \frac{1}{\Pi^*} \int_0^{a^+} \bar{\beta}(a) [\eta_L y^*(a) + z^*(a) + \eta_T u^*(a) + \eta_A v^*(a)] da = \mathcal{H}(\Pi^*).$$

Since $\eta_L, \eta_T, \eta_A \in (0, 1)$, $\eta_L y^*(a) + z^*(a) + \eta_T u^*(a) + \eta_A v^*(a) < 1$, then we have

$$\begin{aligned} \mathcal{H}(\Pi^*) &= \frac{1}{\Pi^*} \int_0^{a^+} \bar{\beta}(a) [\eta_L y^*(a) + z^*(a) + \eta_T u^*(a) + \eta_A v^*(a)] da \\ &\leq \frac{\int_0^{a^+} \bar{\beta}(a) da}{\Pi^*}. \end{aligned} \tag{17}$$

The right-hand side of (17) approaches zero as Π^* approaches infinity; therefore, $\mathcal{H}(\Pi^*) = 1$ has a unique solution in $(0, +\infty)$. Furthermore, if $\Pi^* \geq \int_0^{a^+} \bar{\beta}(a) da$, then $\mathcal{H}(\Pi^*) < 1$, hence, (17) has a unique solution in $(0, \int_0^{a^+} \bar{\beta}(a) da)$. Thus, a disease-endemic equilibrium exists. \square

Now, we study the stability of E^* for system (3). Let $\hat{x}(a, t), \hat{y}(a, t), \hat{z}(a, t), \hat{u}(a, t), \hat{v}(a, t), \hat{w}(a, t)$ be the perturbations of $x^*(a), y^*(a), z^*(a), u^*(a), v^*(a), w^*(a)$, respectively, and set

$$\begin{aligned} \hat{x}(a, t) &= \hat{x}(a)e^{\ell t}, \hat{y}(a, t) = \hat{y}(a)e^{\ell t}, \hat{z}(a, t) = \hat{z}(a)e^{\ell t}, \\ \hat{u}(a, t) &= \hat{u}(a)e^{\ell t}, \hat{v}(a, t) = \hat{v}(a)e^{\ell t}, \hat{w}(a, t) = \hat{w}(a)e^{\ell t}. \end{aligned} \tag{18}$$

We have the following equations

$$\left\{ \begin{aligned} \frac{d\hat{x}}{da} &= -\ell\hat{x}(a) + \theta(a)\hat{w}(a) - \psi(a)\hat{x}(a) - B(a)\widehat{\Pi}x^*(a) - B(a)\Pi^*\hat{x}(a), \\ \frac{d\hat{y}}{da} &= -\ell\hat{y}(a) + B(a)\widehat{\Pi}x^*(a) + B(a)\Pi^*\hat{x}(a) - \phi(a)\hat{y}(a), \\ \frac{d\hat{z}}{da} &= -\ell\hat{z}(a) + \phi(a)\hat{y}(a) - r\hat{z}(a), \\ \frac{d\hat{u}}{da} &= -\ell\hat{u}(a) + \omega(a)r\hat{z}(a) - \alpha(a)\hat{u}(a), \\ \frac{d\hat{v}}{da} &= -\ell\hat{v}(a) + (1 - \omega(a))r\hat{z}(a) + \alpha(a)\hat{u}(a), \\ \frac{d\hat{w}}{da} &= -\ell\hat{w}(a) + \psi(a)\hat{x}(a) - \theta(a)\hat{w}(a), \end{aligned} \right. \tag{19}$$

where $\widehat{\Pi} = \int_0^{a^+} \bar{\beta}(a) (\eta_L \hat{y}(a) + \hat{z}(a) + \eta_T \hat{u}(a) + \eta_A \hat{v}(a)) da$, with the initial conditions

$$\hat{x}(0) = \hat{y}(0) = \hat{z}(0) = \hat{u}(0) = \hat{v}(0) = \hat{w}(0) = 0.$$

Assume that $\widehat{\Pi} \neq 0$ and let

$$x = \frac{\hat{x}}{\widehat{\Pi}}, \quad y = \frac{\hat{y}}{\widehat{\Pi}}, \quad z = \frac{\hat{z}}{\widehat{\Pi}}, \quad u = \frac{\hat{u}}{\widehat{\Pi}}, \quad v = \frac{\hat{v}}{\widehat{\Pi}}, \quad w = \frac{\hat{w}}{\widehat{\Pi}},$$

then system (19) becomes

$$\left\{ \begin{array}{l} \frac{dx}{da} = -\ell x(a) + \theta(a)w(a) - \psi(a)x(a) - B(a)x^*(a) - B(a)\Pi^*x(a), \\ \frac{dy}{da} = -\ell y(a) + B(a)x^*(a) + B(a)\Pi^*x(a) - \phi(a)y(a), \\ \frac{dz}{da} = -\ell z(a) + \phi(a)\hat{y}(a) - r\hat{z}(a), \\ \frac{du}{da} = -\ell u(a) + \omega(a)rz(a) - \alpha(a)u(a), \\ \frac{dv}{da} = -\ell v(a) + (1 - \omega(a))rz(a) + \alpha(a)u(a), \\ \frac{dw}{da} = -\ell w(a) + \psi(a)x(a) - \theta(a)w(a), \end{array} \right. \tag{20}$$

with the initial conditions

$$x(0) = y(0) = z(0) = u(0) = v(0) = w(0) = 0.$$

From (20), we obtain that

$$1 = \int_0^{a+} \bar{\beta}(a) \left(\eta_L y(a) + z(a) + \eta_T u(a) + \eta_A v(a) \right) da. \tag{21}$$

Denote the right-hand of (21) by $\mathcal{L}(\ell)$, then we have the following proposition:

Proposition 1 $\mathcal{L}(\ell)$ is a decreasing function of ℓ , which approaches zero as $\ell \rightarrow \infty$ and $\mathcal{L}(0) < 1$.

Proof From system (20), we get

$$\left\{ \begin{array}{l} x(a) = \int_0^a \left(\theta(\eta) - B(\eta)x^*(\eta) \right) \exp \left\{ - \int_\eta^a \left(\ell + \psi(\xi) + B(\xi)\Pi^* \right) d\xi \right\} d\eta, \\ y(a) = \int_0^a \left(B(\eta)x^*(\eta) + B(\eta)\Pi^*x(\eta) \right) \exp \left\{ - \int_\eta^a \left(\ell + \phi(\xi) \right) d\xi \right\} d\eta, \\ z(a) = \int_0^a \phi(\eta)y(\eta)e^{-(\ell+r)(a-\eta)}d\eta, \\ u(a) = \int_0^a \omega(\eta)rz(\eta) \exp \left\{ - \int_\eta^a \left(\ell + \alpha(\xi) \right) d\xi \right\} d\eta, \\ v(a) = \int_0^a \left((1 - \omega(\eta))rz(\eta) + \alpha(\eta)u(\eta) \right) e^{-\ell(a-\eta)}d\eta, \\ w(a) = \int_0^a \psi(\eta)x(\eta) \exp \left\{ - \int_\eta^a \left(\ell + \theta(\xi) \right) d\xi \right\} d\eta, \end{array} \right. \quad (22)$$

that gives

$$\begin{aligned} \mathcal{L}(\ell) &= \int_0^{a+} \bar{\beta}(a) \left(\eta_L y(a) + z(a) + \eta_T u(a) + \eta_A v(a) \right) da \\ &= \int_0^{a+} \bar{\beta}(a) \left\{ \eta_L y(a) + \int_0^a \phi(\eta)y(\eta)e^{-(\ell+r)(a-\eta)}d\eta \right. \\ &\quad \left. + \eta_T \int_0^a \omega(\eta)rz(\eta) \exp \left\{ - \int_\eta^a \left(\ell + \alpha(\xi) \right) d\xi \right\} d\eta \right. \\ &\quad \left. + \eta_A \int_0^a \left((1 - \omega(\eta))rz(\eta) + \alpha(\eta)u(\eta) \right) e^{-\ell(a-\eta)}d\eta \right\} da. \end{aligned} \quad (23)$$

Consider $y(a) > 0$; therefore, from (23) we see that $\mathcal{L}(\ell)$ decreases in ℓ and $\mathcal{L}(\ell)$ approaches 0 as ℓ approaches ∞ .

Next, we prove $\mathcal{L}(0) < 1$. We rewrite $y(a)$ in system (22) as follows:

$$y(a) = y_1(a) + y_2(a),$$

where

$$\begin{aligned} y_1(a) &= \int_0^a B(\eta)x^*(\eta) \exp \left\{ - \int_\eta^a \left(\ell + \phi(\xi) \right) d\xi \right\} d\eta, \\ y_2(a) &= \int_0^a B(\eta)\Pi^*x(\eta) \exp \left\{ - \int_\eta^a \left(\ell + \phi(\xi) \right) d\xi \right\} d\eta. \end{aligned}$$

Then,

$$\begin{aligned}
 z_i(a) &= \int_0^a \phi(\eta)y_i(\eta) \exp \left\{ - \int_\eta^a (\ell + r)d\xi \right\} d\eta, \\
 u_i(a) &= \int_0^a \omega(\eta)r z_i(\eta) \exp \left\{ - \int_\eta^a (\ell + \alpha(\xi))d\xi \right\} d\eta, \\
 v_i(a) &= \int_0^a \left((1 - \omega(\eta))r z_i(\eta) + \alpha(\eta)u_i(\eta) \right) e^{-\ell(a-\eta)} d\eta, \quad i = 1, 2.
 \end{aligned}$$

Hence, \mathcal{L} can be written

$$\mathcal{L}(\ell) = \mathcal{L}_1(\ell) + \mathcal{L}_2(\ell),$$

where

$$\begin{aligned}
 \mathcal{L}_i(\ell) &= \int_0^{a+} \bar{\beta}(a) \left\{ \eta_L y_i(a) + \int_0^a \phi(\eta)y_i(\eta)e^{-(\ell+r)(a-\eta)} d\eta \right. \\
 &\quad + \eta_T \int_0^a \omega(\eta)r z_i(\eta) \exp \left\{ - \int_\eta^a (\ell + \alpha(\xi))d\xi \right\} d\eta \\
 &\quad \left. + \eta_A \int_0^a \left((1 - \omega(\eta))r z_i(\eta) + \alpha(\eta)u_i(\eta) \right) e^{-\ell(a-\eta)} d\eta \right\} da, \quad i = 1, 2.
 \end{aligned} \tag{24}$$

Obviously, $\mathcal{L}_1(0) + \mathcal{L}_2(0) = \mathcal{R}(\psi, \theta) + \mathcal{L}_2(0) = 1 + \mathcal{L}_2(0)$. Furthermore, let $q(a) = x(a) + y(a) + z(a) + u(a) + v(a)$. From (20), we have $q(a) = - \int_0^a \omega(\eta)z(\eta)e^{-\ell(a-\eta)} d\eta < 0$. Since $\eta_L y(a) + z(a) + \eta_T u(a) + \eta_A v(a) > 0$, which implies $y(a) + z(a) + u(a) + v(a) > 0$, we have $x(a) < 0$. Hence, from (20), $\mathcal{L}_2(0) < 0$ is obtained. Finally, the proof of $\mathcal{L}(0) < 1$ is complete. Hence, we have the following result. □

Theorem 6.2 *If $d(a) = 0$ and $\mathcal{R}(\psi, \theta) > 1$, then the disease-endemic steady-state E^* of system (2) is stable.*

7 The Demographic Model with Age Groups

In this section, we will study the demographic version of the model (1) without PrEP interventions. First, we divide the population into n age groups. The subscript k represents the parts of the epidemiological classes in the i th age interval $[a_{i-1}, a_i]$, with $W_i(t) = \int_{a_{i-1}}^{a_i} W(a, t) da$, where $W = S, L, I, T, A$. Suppose the population is growing exponentially by e^{bt} and apply the method mentioned in Hethcote (2000), then we obtain the following system of differential equations

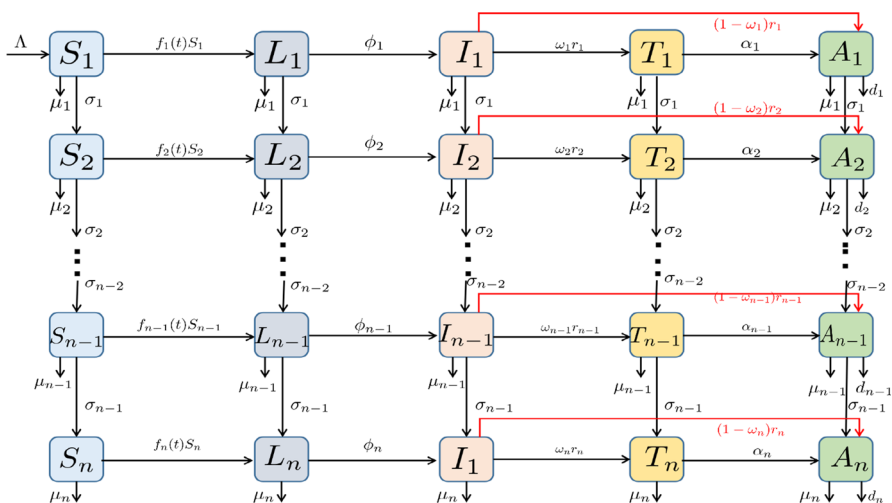


Fig. 3 Schematic diagram of the demographic model (25)

$$\left\{ \begin{array}{l} \frac{dS_1}{dt} = \Lambda - f_1(t)S_1 - (\mu_1 + \sigma_1)S_1, \\ \frac{dS_i}{dt} = \sigma_{i-1}S_{i-1} - f_i(t)S_i - (\mu_i + \sigma_i)S_i, \quad 2 \leq i \leq n, \\ \frac{dL_1}{dt} = f_1(t)S_1 - (\mu_1 + \sigma_1 + \phi_1)L_1, \\ \frac{dL_i}{dt} = f_i(t)S_i + \sigma_{i-1}L_{i-1} - (\mu_i + \sigma_i + \phi_i)L_i, \quad 2 \leq i \leq n, \\ \frac{dI_1}{dt} = \phi_1L_1 - (\mu_1 + r_1 + \sigma_1)I_1, \\ \frac{dI_i}{dt} = \sigma_{i-1}I_{i-1} + \phi_iL_i - (\mu_i + r_i + \sigma_i)I_i, \quad 2 \leq i \leq n, \\ \frac{dT_1}{dt} = \omega_1r_1I_1 - (\mu_1 + \alpha_1 + \sigma_1)T_1, \\ \frac{dT_i}{dt} = \sigma_{i-1}T_{i-1} + \omega_i r_i I_i - (\mu_i + \alpha_i + \sigma_i)T_i, \quad 2 \leq i \leq n, \\ \frac{dA_1}{dt} = \alpha_1T_1 + (1 - \omega_1)r_1I_1 - (\mu_1 + d_1 + \sigma_1)A_1, \\ \frac{dA_i}{dt} = \sigma_{i-1}A_{i-1} + \alpha_iT_i + (1 - \omega_i)r_iI_i - (\mu_i + d_i + \sigma_i)A_i, \quad 2 \leq i \leq n, \end{array} \right. \tag{25}$$

where $f_i(t) = \beta_i \sum_{k=1}^n \eta_{ki}(e_k L_k + I_k + b_k T_k + c_k A_k) / N_k$, $i = 1, 2, \dots, n$. The diagram of model (25) is shown in Fig. 3.

7.1 The Basic Reproduction Number

In this subsection, we derive the basic reproduction number R_0 of the system (25). In fact, system (25) always has a disease-free equilibrium

$$E_0 = (\mathbf{S}^0, \mathbf{L}^0, \mathbf{I}^0, \mathbf{T}^0, \mathbf{A}^0),$$

where

$$S_1^0 = \frac{\Lambda}{\mu_1 + \sigma_1}, S_i^0 = \frac{\sigma_{i-1}S_{i-1}^0}{\mu_i + \sigma_i}, L_i^0 = I_i^0 = T_i^0 = A_i^0 = 0, 1 \leq i \leq n.$$

Thus, the linearized system with infection compartments around E_0 is given by

$$\left\{ \begin{aligned} \frac{dL_1}{dt} &= \beta_1 \sum_{k=1}^n \eta_{k1}(e_k L_k + I_k + b_k T_k + c_k A_k) - (\mu_1 + \sigma_1 + \phi_1)L_1, \\ \frac{dL_i}{dt} &= \beta_i \sum_{k=1}^n \eta_{ki}(e_k L_k + I_k + b_k T_k + c_k A_k) + \sigma_{i-1}L_{i-1} - (\mu_i + \sigma_i + \phi_i)L_i, \\ & \quad 2 \leq i \leq n, \\ \frac{dI_1}{dt} &= \phi_1 L_1 - (\mu_1 + r_1 + \sigma_1)I_1, \\ \frac{dI_i}{dt} &= \sigma_{i-1}I_{i-1} + \phi_i L_i - (\mu_i + \gamma_i + \sigma_i)I_i, 2 \leq i \leq n, \\ \frac{dT_1}{dt} &= \omega_1 r_1 I_1 - (\mu_1 + \alpha_1 + \sigma_1)T_1, \\ \frac{dT_i}{dt} &= \sigma_{i-1}T_{i-1} + \omega_i \gamma_i I_i - (\mu_i + \alpha_i + \sigma_i)T_i, 2 \leq i \leq n, \\ \frac{dA_1}{dt} &= \alpha_1 T_1 + (1 - \omega_1)\gamma_1 I_1 - (\mu_1 + d_1 + \sigma_1)A_1, \\ \frac{dA_i}{dt} &= \sigma_{i-1}A_{i-1} + \alpha_i T_i + (1 - \omega_i)\gamma_i I_i - (\mu_i + d_i + \sigma_i)A_i, 2 \leq i \leq n. \end{aligned} \right. \tag{26}$$

Let $x = (\mathbf{L}, \mathbf{I}, \mathbf{T}, \mathbf{A})^T$, then system (26) can be rewritten as

$$\frac{dx}{dt} = (\mathcal{F} - \mathcal{V})x,$$

where

$$\mathcal{F} = \begin{bmatrix} H_{11} & H_{12} & H_{13} & H_{14} \\ 0 & 0 & 0 & 0 \\ 0 & 0 & 0 & 0 \\ 0 & 0 & 0 & 0 \end{bmatrix}, \mathcal{V} = \begin{bmatrix} V_{11} & 0 & 0 & 0 \\ V_{21} & V_{22} & 0 & 0 \\ 0 & V_{32} & V_{33} & 0 \\ 0 & V_{42} & 0 & V_{44} \end{bmatrix},$$

with

$$\begin{aligned}
 H_{11} &= \begin{bmatrix} \beta_1 \eta_{11} e_1 & \beta_1 \eta_{12} e_2 & \cdots & \beta_1 \eta_{1n} e_n \\ \beta_2 \eta_{21} e_1 & \beta_2 \eta_{22} e_2 & \cdots & \beta_2 \eta_{2n} e_n \\ \vdots & \vdots & \ddots & \vdots \\ \beta_n \eta_{n1} e_1 & \beta_n \eta_{n2} e_2 & \cdots & \beta_n \eta_{nn} e_n \end{bmatrix}, H_{12} = \begin{bmatrix} \beta_1 \eta_{11} & \beta_1 \eta_{12} & \cdots & \beta_1 \eta_{1n} \\ \beta_2 \eta_{21} & \beta_2 \eta_{22} & \cdots & \beta_2 \eta_{2n} \\ \vdots & \vdots & \ddots & \vdots \\ \beta_n \eta_{n1} & \beta_n \eta_{n2} & \cdots & \beta_n \eta_{nn} \end{bmatrix}, \\
 H_{13} &= \begin{bmatrix} \beta_1 \eta_{11} b_1 & \beta_1 \eta_{12} b_2 & \cdots & \beta_1 \eta_{1n} b_n \\ \beta_2 \eta_{21} b_1 & \beta_2 \eta_{22} b_2 & \cdots & \beta_2 \eta_{2n} b_n \\ \vdots & \vdots & \ddots & \vdots \\ \beta_n \eta_{n1} b_1 & \beta_n \eta_{n2} b_2 & \cdots & \beta_n \eta_{nn} b_n \end{bmatrix}, H_{14} = \begin{bmatrix} \beta_1 \eta_{11} c_1 & \beta_1 \eta_{12} c_2 & \cdots & \beta_1 \eta_{1n} c_n \\ \beta_2 \eta_{21} c_1 & \beta_2 \eta_{22} c_2 & \cdots & \beta_2 \eta_{2n} c_n \\ \vdots & \vdots & \ddots & \vdots \\ \beta_n \eta_{n1} c_1 & \beta_n \eta_{n2} c_2 & \cdots & \beta_n \eta_{nn} c_n \end{bmatrix}, \\
 V_{11} &= \begin{bmatrix} \mu_1 + \sigma_1 + \phi_1 & 0 & \cdots & 0 & 0 \\ -\sigma_1 & \mu_2 + \sigma_2 + \phi_2 & \cdots & 0 & 0 \\ \vdots & \vdots & \ddots & \vdots & \vdots \\ 0 & 0 & \cdots & -\sigma_{n-1} & \mu_n + \sigma_n + \phi_n \end{bmatrix}, \\
 V_{21} &= \begin{bmatrix} -\phi_1 & 0 & \cdots & 0 \\ 0 & -\phi_2 & \cdots & 0 \\ \vdots & \vdots & \ddots & \vdots \\ 0 & 0 & \cdots & -\phi_n \end{bmatrix}, \\
 V_{22} &= \begin{bmatrix} \mu_1 + \sigma_1 + r_1 & 0 & \cdots & 0 & 0 \\ -\sigma_1 & \mu_2 + \sigma_2 + r_2 & \cdots & 0 & 0 \\ \vdots & \vdots & \ddots & \vdots & \vdots \\ 0 & 0 & \cdots & -\sigma_{n-1} & \mu_n + \sigma_n + r_n \end{bmatrix}, \\
 V_{32} &= \begin{bmatrix} -\omega_1 r_1 & 0 & \cdots & 0 \\ 0 & -\omega_2 r_2 & \cdots & 0 \\ \vdots & \vdots & \ddots & \vdots \\ 0 & 0 & \cdots & -\omega_n r_n \end{bmatrix}, \\
 V_{33} &= \begin{bmatrix} \mu_1 + \sigma_1 + \alpha_1 & 0 & \cdots & 0 & 0 \\ -\sigma_1 & \mu_2 + \sigma_2 + \alpha_2 & \cdots & 0 & 0 \\ \vdots & \vdots & \ddots & \vdots & \vdots \\ 0 & 0 & \cdots & -\sigma_{n-1} & \mu_n + \sigma_n + \alpha_n \end{bmatrix}, \\
 V_{42} &= \begin{bmatrix} -(1 - \omega_1) r_1 & 0 & \cdots & 0 \\ 0 & -(1 - \omega_2) r_2 & \cdots & 0 \\ \vdots & \vdots & \ddots & \vdots \\ 0 & 0 & \cdots & -(1 - \omega_n) r_n \end{bmatrix}, \\
 V_{44} &= \begin{bmatrix} \mu_1 + \sigma_1 + d_1 & 0 & \cdots & 0 & 0 \\ -\sigma_1 & \mu_2 + \sigma_2 + d_2 & \cdots & 0 & 0 \\ \vdots & \vdots & \ddots & \vdots & \vdots \\ 0 & 0 & \cdots & -\sigma_{n-1} & \mu_n + \sigma_n + d_n \end{bmatrix}.
 \end{aligned}$$

From Feng et al. (2020), we can obtain the basic reproduction number R_0 of system (25) as follows:

$$R_0 = \rho \left(\mathcal{F} \mathcal{V}^{-1} \right). \tag{27}$$

7.2 Fitting Model (25) to the HIV/AIDS Reported Data in China

In this subsection, applying the MCMC method mentioned in (Xue et al. 2022, subsection 3.2) we first estimate some model parameters and initial values of system (25) based on the yearly number of newly reported HIV/AIDS cases for 11 age groups from 2004 to 2018 in China. The corresponding collection of real data is given in ‘‘Appendix A’’.

7.2.1 Parameter Estimation

To simulate the number of HIV/AIDS reported cases in mainland China, the rationality of the model is verified by the newly infected real cases. Here, the total population is divided into 11 age groups and transmission only happened through sexual behaviors. The values of some model parameters are estimated as follows:

1. Similar to Zheng et al. (2021), we assume that the recruitment rate of $S_1(t)$ is $\Lambda = N_1 \times \mu_1$.
2. Since the maximum difference of age for each age group is five years, we choose

$$\sigma_i = \begin{cases} \frac{1}{5}, & 1 \leq i \leq 10, \\ 0, & i = 11. \end{cases}$$

3. Since the window period of HIV is generally 2–4 weeks, up to 6 months (Sweeting and Angelis 2010), the value of ϕ_i is obtained by data fitting, $i = 1, 2, \dots, 11$.
4. From literature (Wu et al. 2020b), we can estimate the proportion of HIV-infected individuals who take ART treatment (ω_i) by data fitting, and we choose ART treatment failure rate (α_i) as

$$\alpha_i = \begin{cases} [5\%, 10\%], & 1 \leq i \leq 10, \\ [15\%, 30\%], & i = 11. \end{cases}$$

5. From China Statistical Yearbook (National Bureau of Statistics 2021), we know that the average lifetime of Chinese people is 76 years; then we can assume that the natural death rate of [0–4] group is $1/76$, under normal circumstances, and that natural morality increases with age. Hence, we can further assume that the natural death rates of [5–9] and [10–14] groups are $1/71$ and $1/66$, respectively (Xue et al. 2022). Thus, we can choose the average lifetime of Chinese as $\mu_1 = 1/61$, $\mu_2 = 1/56$, $\mu_3 = 1/51$, $\mu_4 = 1/46$, $\mu_5 = 1/41$, $\mu_6 = 1/36$, $\mu_7 = 1/31$, $\mu_8 = 1/26$, $\mu_9 = 1/21$, $\mu_{10} = 1/16$, $\mu_{11} = 1/12$.

Table 2 Death rate due to AIDS in different age groups with data from Data-Center of China Public Health Science (2021)

Age group	15–19	20–24	25–29	30–34	35–39	40–44
AIDS death rate	0.103	0.134	0.125	0.135	0.162	0.143
Age group	45–49	50–54	55–59	60–64	65+	
AIDS death rate	0.152	0.169	0.183	0.219	0.305	

- Based on the statistical data in Data-Center of China Public Health Science (2021), the average death rate d_i ($i = 1, 2, \dots, 11$) due to AIDS in different age groups is listed in Table 2.
- We obtain the total population of the i -th age group as N_i . According to a recent report, more than 1.05 million people are infected with HIV in China; therefore, we can approximate the initial values as $L_i(0) = 1.05$. $I_i(0) =$ new cases, $A_i(0) =$ new cases, $T_i(0)$ can be estimated by fitting with the data, and $S_i(0) = N_i - L_i(0) - I_i(0) - T_i(0) - A_i(0)$, $i = 1, 2, \dots, 11$.
- The values of γ_i and β_i are obtained by fitting with the data, $i = 1, 2, \dots, 11$.
- The values of b_i and c_i , the coefficients that describe reduction in the transmission rate due to ART treatment, are obtained by fitting with the data, $i = 1, 2, \dots, 11$.
- The contact matrix (i.e., $(\eta_{ki})_{n \times n}$): We aggregate it into 14 age groups by using the method mentioned in Xue et al. (2022). Specifically, we set \bar{B} as the known contact matrix, as displayed in Appendix B.4 in Xue et al. (2022), and \bar{b}_{ig} , $i, g = 1, 2, \dots, m$, represents the elements in the contact matrix, where m is the number of age groups and i, j , respectively, represent the rows and columns in the matrix. We denote $C=(c_{kj})$, $k, j = 1, 2, \dots, n$, as the modified contact matrix, then we set age group \bar{v} containing narrower age groups $i = l(k)$ to $g(k)$. Then the contact rate between i group and g group can be given by $\bar{d}_{i,j} = \sum_{g=k(j)}^{\bar{v}(j)} \bar{b}_{ig}$. Furthermore, the total number of contact from k to j and from j to k is given by $\bar{Y}_{kj} = \sum_{i=l(k)}^{\bar{v}(k)} N_i \bar{d}_{ij}$ and $\bar{Y}_{jk} = \sum_{i=l(j)}^{\bar{v}(j)} N_i \bar{d}_{ik}$, respectively, where N_i represents the population in age group i (see Appendix B.5 in Xue et al. 2022). To ensure that $\bar{Y}_{kj} = \bar{Y}_{jk}$, we set $W_{kj} = W_{jk} = (\bar{Y}_{kj} + \bar{Y}_{jk})/2$. Finally, the modified contact matrix elements are given by $c_{kj} = \frac{W_{kj}}{\sum_{i=l(k)}^{\bar{v}(k)} N_i}$, $c_{jk} = \frac{W_{jk}}{\sum_{i=l(j)}^{\bar{v}(j)} N_i}$ and the total contact rate on the diagonal is given by $c_{kk} = \frac{\sum_{i=l(k)}^{\bar{v}(k)} N_i \bar{d}_{ik}}{\sum_{i=l(k)}^{\bar{v}(k)} N_i}$. The modified contact matrix is shown in Fig. 4. We use the modified contact matrix C to approximate the contact matrix $(\eta_{ki})_{n \times n}$ in the simulation.

Based on the parameter estimations mentioned above, the fitted curves of new and cumulative HIV/AIDS cases for the 15–19 age group are presented in Fig. 5. The collection of the other fitted curves is presented in “Appendix B”. It can be seen that model (25) fits the new and cumulative cases in the 11 age groups reasonably well.

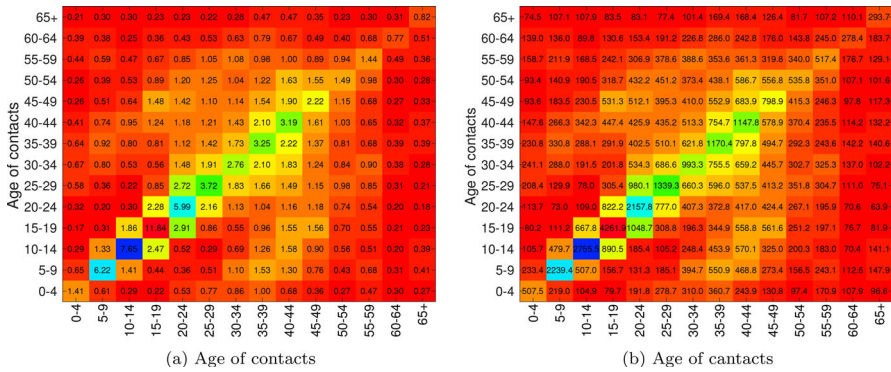


Fig. 4 **a** Contact number of each individual in 14 age groups per day; **b** contact number of each individual in 14 age groups per year

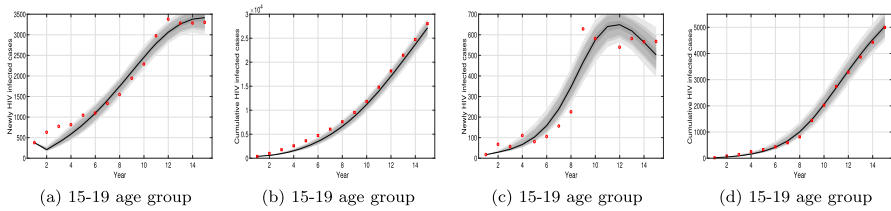


Fig. 5 Fitting curves of the new and cumulative HIV and AIDS reported cases for the 15–19 age group from 2004 to 2018

7.3 The Sensitivity Analysis

From the fitting results, we can obtain the values of estimated parameters by the MCMC method as shown in Table 3. Based on the estimated parameter values, the mean of the basic reproduction number R_0 is 1.7955 with 95% confidence interval (1.791, 1.802), which is shown in Fig. 6.

To study the effects of the parameters on R_0 of system (25), we perform sensitivity analysis by Latin square sampling and partial rank correlation coefficient (PRCC) methods. In the absence of available data on the distribution functions, we choose a uniform distribution for all input parameters as shown in Table 3 and tested for significant PRCCs for all parameters of R_0 . The corresponding outcome is given in Fig. 7.

As can be seen from Fig. 7, R_0 is positively and negatively correlated with parameters $\beta_i, \omega_i, b_i, c_i, e_i$ ($1 \leq i \leq 11$) and $\gamma_i, \alpha_i, \phi_i$, respectively. This shows that the increase in the values of parameters $\beta_i, \omega_i, b_i, c_i, e_i$ will significantly increase the risk of disease transmission, and the increase in the values of parameters $\gamma_i, \alpha_i, \phi_i$ will effectively reduce the risk of disease transmission. Furthermore, the parameters in the older group have a less significant effect on R_0 , which means that the older age groups have more severe HIV complications than the other age groups. Therefore, we need to focus on more effective HIV transmission prevention and control measures for adolescents (15–24) and adults (25–49).

Table 3 Values of some estimated parameters by the MCMC method

ϕ_1	0.108	β_1	1.064×10^{-9}	ω_1	0.125	e_1	0.377
ϕ_2	0.398	β_2	4.294×10^{-9}	ω_2	0.022	e_2	0.023
ϕ_3	0.194	β_3	2.64×10^{-9}	ω_3	0.077	e_3	0.344
ϕ_4	0.643	β_4	1.265×10^{-8}	ω_4	0.004	e_4	0.002
ϕ_5	0.528	β_5	7.95×10^{-9}	ω_5	0.007	e_5	0.003
ϕ_6	0.607	β_6	9.95×10^{-9}	ω_6	0.012	e_6	0.007
ϕ_7	0.310	β_7	5.39×10^{-9}	ω_7	0.026	e_7	0.030
ϕ_8	0.612	β_8	9.77×10^{-9}	ω_8	0.017	e_8	0.007
ϕ_9	0.549	β_9	5.74×10^{-9}	ω_9	0.016	e_9	0.340
ϕ_{10}	0.239	β_{10}	4.314×10^{-9}	ω_{10}	0.038	e_{10}	0.018
ϕ_{11}	0.850	β_{11}	7.82×10^{-9}	ω_{11}	0.057	e_{11}	0.016
b_1	0.718	c_1	0.495	α_1	0.064	γ_1	0.552
b_2	0.738	c_2	0.479	α_2	0.074	γ_2	0.350
b_3	0.204	c_3	0.408	α_3	0.090	γ_3	0.572
b_4	0.804	c_4	0.050	α_4	0.069	γ_4	0.546
b_5	0.768	c_5	0.121	α_5	0.076	γ_5	0.529
b_6	0.170	c_6	0.061	α_6	0.091	γ_6	0.424
b_7	0.134	c_7	0.174	α_7	0.100	γ_7	0.664
b_8	0.024	c_8	0.027	α_8	0.050	γ_8	0.407
b_9	0.102	c_9	0.206	α_9	0.085	γ_9	0.562
b_{10}	0.109	c_{10}	0.234	α_{10}	0.095	γ_{10}	0.649
b_{11}	0.020	c_{11}	0.089	α_{11}	0.162	γ_{11}	0.670

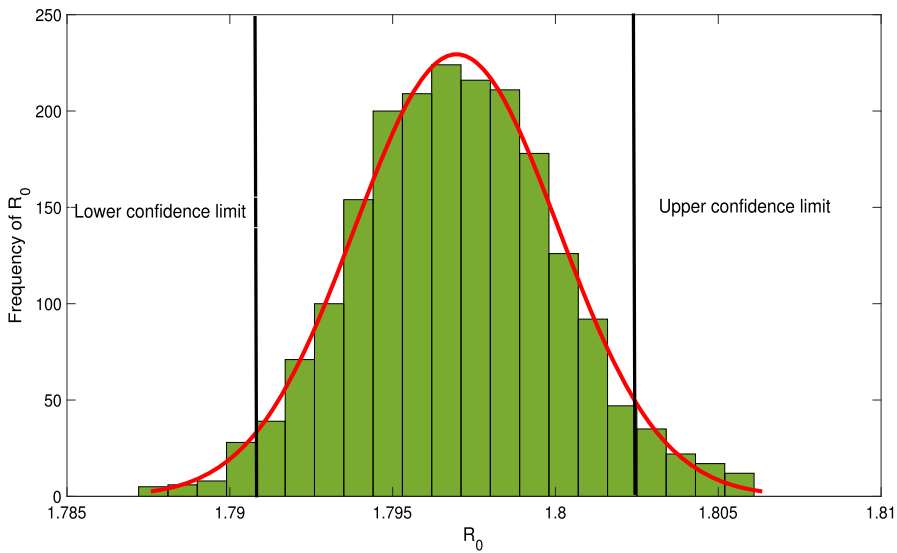


Fig. 6 Frequency of R_0 , the red curve is the probability density function curve of R_0 (Color figure online)

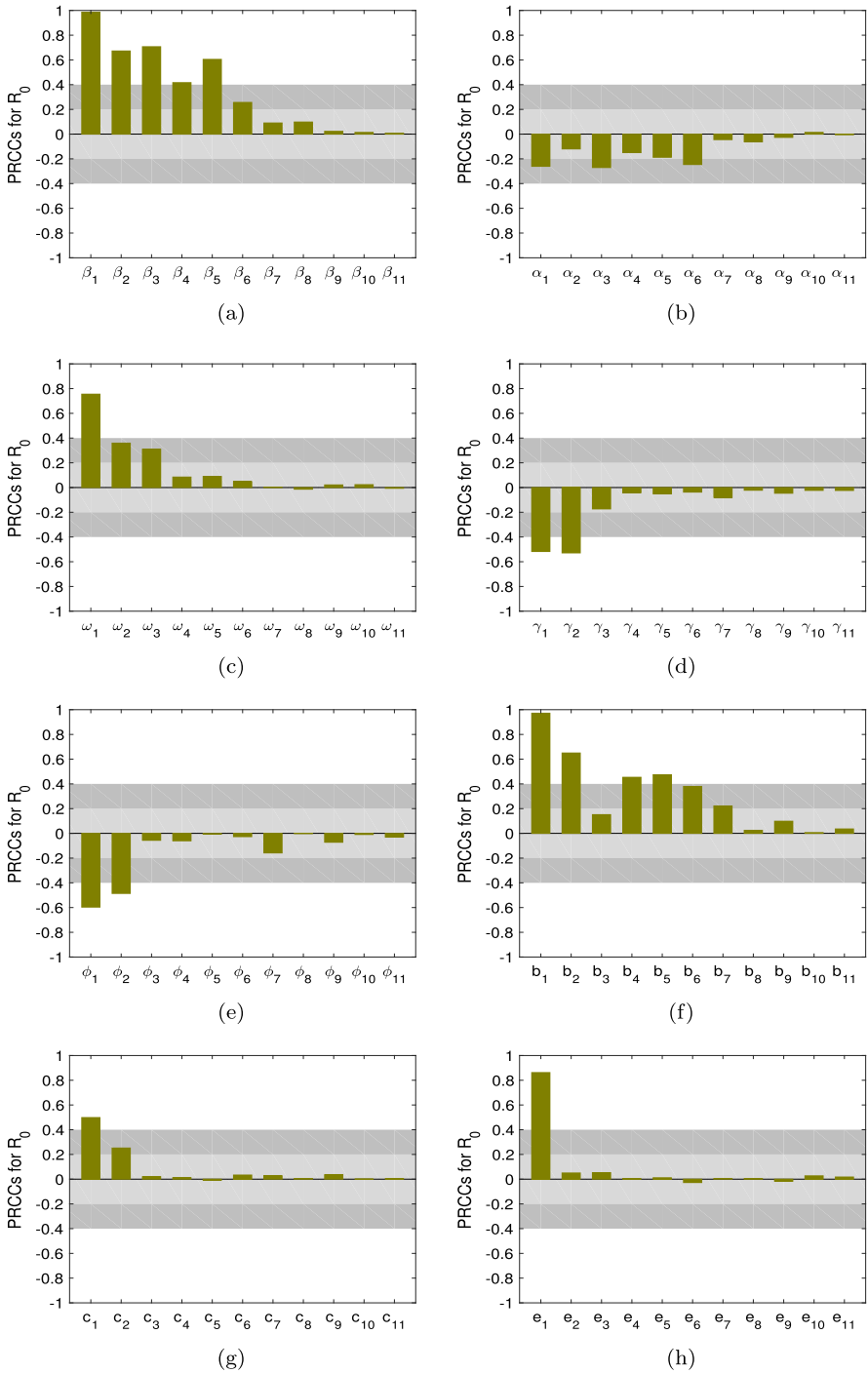


Fig. 7 PRCC of R_0 for some model parameters

Table 4 Values of the basic reproduction number R_0^i for the i -th group, $i = 1, 2, \dots, 11$

Group	1	2	3	4	5	6	7	8	9	10	11
R_0^i	1.430	1.572	1.509	1.412	1.504	1.390	1.422	1.494	1.544	1.486	2.11

Next, we discuss the different contribution to the disease from each age group. To this end, according to Gao et al. (2022), we define the basic reproduction number of group i as

$$R_0^i = \rho(\mathcal{F}_i \mathcal{V}^{-1}),$$

where $\sigma_i = 0$ in \mathcal{V} and

$$\mathcal{F}_i = \begin{bmatrix} e_i H_i & H_i & b_i H_i & c_i H_i \\ 0 & 0 & 0 & 0 \\ 0 & 0 & 0 & 0 \\ 0 & 0 & 0 & 0 \end{bmatrix},$$

with

$$H_1 = \begin{bmatrix} \beta_1 \eta_{11} & 0 & \dots & 0 \\ \beta_2 \eta_{21} & 0 & \dots & 0 \\ \vdots & \vdots & \vdots & \vdots \\ \beta_n \eta_{n1} & 0 & \dots & 0 \end{bmatrix}, H_k = \begin{bmatrix} 0 & \dots & \beta_1 \eta_{1k} & \dots & 0 \\ 0 & \dots & \beta_2 \eta_{2k} & \dots & 0 \\ \vdots & \vdots & \vdots & \vdots & \vdots \\ 0 & \dots & \beta_n \eta_{nk} & \dots & 0 \end{bmatrix}, H_n = \begin{bmatrix} 0 & \dots & 0 & \beta_1 \eta_{1n} \\ 0 & \dots & 0 & \beta_2 \eta_{2n} \\ \vdots & \vdots & \vdots & \vdots \\ 0 & \dots & 0 & \beta_n \eta_{nn} \end{bmatrix},$$

where $2 \leq k \leq n - 1$. Thus, based on the estimated values of parameters in subsection 7.2.1 and Table 3, after some calculations, we can obtain the values of the basic reproduction number R_0^i for the i -th group, which are all listed in Table 4.

From Table 4, we can see that there are significant differences in the values of the basic reproduction number R_0^i among different age groups. In particular, the value of the basic reproduction number 1.430–1.572 of the young age group 20–29 and the value of basic reproduction number 2.11 of the elder group 65+ are close to the numerical results in Zhao et al. (2020) (the estimated values of the basic reproduction number of these two age groups in Zhao et al. (2020) are 1.65 and 2.25, respectively). Moreover, we can see from Table 4 that the values of the basic reproduction number of the young group and the elder group are higher than those of the other age groups, which reflects the current trend of AIDS transmission in China. This is in line with (Zhao et al. 2020; Qiao and Xu 2019; Zhang and Cai 2020).

8 Numerical Results of System (1)

In this section, we explore model (1) to study the impact of PrEP intervention.

Table 5 Fitting functions of parameters

Parameters	Form	c	k_1	k_2	m
$\mu(a)$	$c + k_1 e^{ma} + k_2 e^{-ma}$	0.0191	3.84×10^{-4}	-0.0136	0.0788
$d(a)$	$c + k_1 e^{ma} + k_2 e^{-ma}$	0.1458	1.307×10^{-5}	-0.3653	0.1446
$\alpha(a)$	$c + k_1 e^{ma} + k_2 e^{-ma}$	0.0760	3.22×10^{-10}	-1.0191	0.2985
$\omega(a)$	$c + k_1 e^{ma} + k_2 e^{-ma}$	0.0183	2.83×10^{-9}	4.6240	0.2535
$\phi(a)$	$c + k_1 e^{ma} + k_2 e^{-ma}$	0.5371	2.40×10^{-10}	-159.335	0.3928
$\beta(a)$	$c(k_1(-(x - 40)^2 + k_2) + m)$ (Kuniya 2017)	2.944×10^{-5}	4.107×10^{-4}	2.1935×10^3	5.720×10^{-2}

8.1 The Numerical Simulation of System (1) Without PrEP Intervention

In this subsection, we attempt to find the numerical simulation of the continuous age-structured model (1) without PrEP intervention $E(a, t)$. In fact, model (25) is transformed from Model (1) under the assumption that some age-dependent parameters follow an exponential distribution. We try to use the fitting results of the model (25) to estimate some age-dependent parameters in the model (1). Therefore, we choose $\mu(a), d(a), \alpha(a), \omega(a), \phi(a)$ as $c + k_1 e^{ma} + k_2 e^{-ma}$, where $a \in [0, a^+]$ with $a_+ = 100$. We give the fitting curves and the values of c, k_1, k_2, m in Fig. 8a–e and Table 5. Moreover, Fig. 4 shows that contact is more likely to occur between individuals of similar age. Based on the values of $\beta_i \sum_{k=1}^{11} \eta_{ki}$ ($1 \leq i \leq 11$) and the numerical method mentioned in Kuniya (2017), we assume $\beta(a) = c(k_1(-(x - 40)^2 + k_2) + m)$ and we obtain the fitting curve and the estimated parameter values of c, k_1, k_2, m , as shown in Fig. 8f and Table 5. For η_L, η_T, η_A , we choose the values of η_L, η_T, η_A as the average values of e_i, b_i and c_i ($1 \leq i \leq 11$), respectively. Thus, applying the method mentioned in Kuniya (2017), Chang and Zhang (2022), Breda et al. (2021), we can calculate the value of $\mathcal{R}_{0,m}$ for each m , as shown in Fig. 9. It can be seen that the error $\mathcal{R}^+ - \mathcal{R}_{0,m}$ (\mathcal{R}^+ represents the reference value of \mathcal{R}_0) converges to 0 as m increases, which implies that $\mathcal{R}_0 \approx 1.8022 > 1$. This result is very close to the value of R_0 (1.7955) of system (25). Hence, we can claim that it is reliable to obtain the value of \mathcal{R}_0 of model (1) by fitting the parameters of system (25).

To verify the rationality and validity of this estimation method, we use model (1) to fit the cumulative HIV/AIDS reported cases from 2004 to 2018 in China. From Fig. 10, we can see that the continuous age-structured model fits the actual reported cases very well. This shows that it is very reasonable to obtain the parameter values of the model by fitting the actual cases of different age groups to model (25) and then estimate the functional form of the age-dependent parameters of model (1) with an exponential distribution. This is also a problem ignored in previous related work: how to use actual reported data to establish an age-structured infectious disease model that can reflect the actual epidemic transmission situation. This numerical scheme can also be extended to other infectious disease models.

We display the dynamical behaviors of the solution for system (1) when $\mathcal{R}_0 = \mathcal{R}(\psi = 0, \theta = 0) > 1$ in Fig. 11. When we choose $c = 1.2 \times 10^{-6}$ in $\beta(a)$, we can obtain that $\mathcal{R}_0 = \mathcal{R}(\psi = 0, \theta = 0) < 1$. In Fig. 12, we can see that the populations

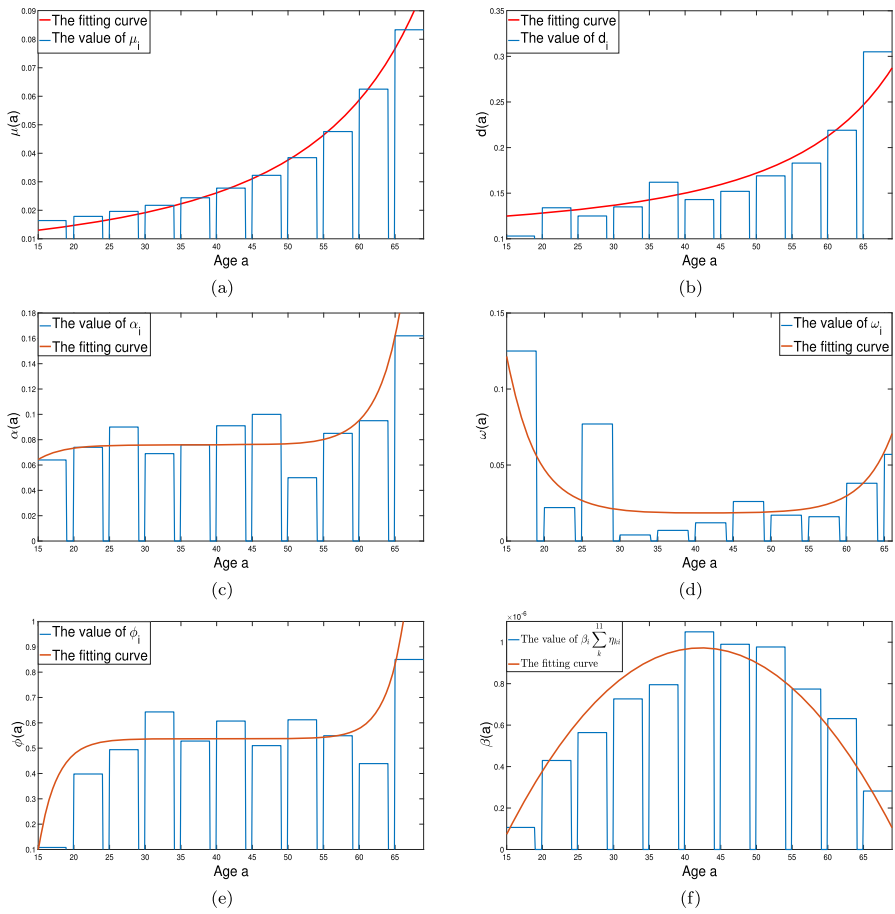


Fig. 8 Fitting curve of some parameters of system (1)

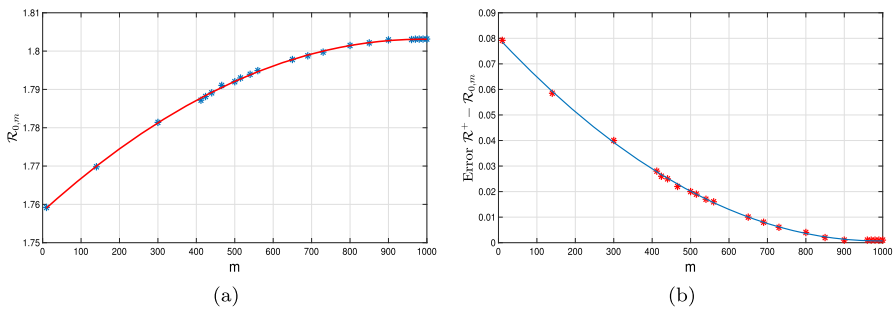


Fig. 9 Value of \mathcal{R}_0 : **a** Plot of the value of $\mathcal{R}_{0,m}$; **b** error $\mathcal{R}^+ - \mathcal{R}_{0,m}$ associated with the reference value \mathcal{R}^+ with respect to \mathcal{R}_0

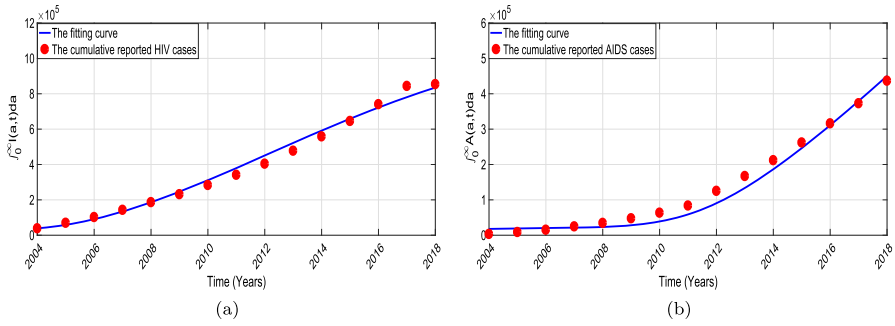


Fig. 10 Fitting curves of the total cumulative HIV/AIDS reported cases from 2004 to 2018 by model (1) in China

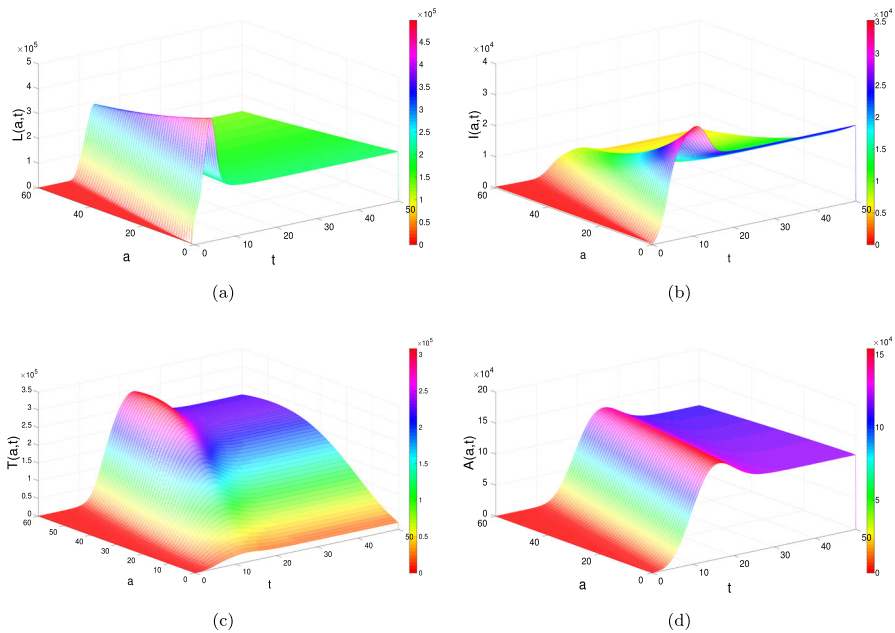


Fig. 11 Dynamical behaviors of the solutions for system (1) when $\mathcal{R}_0 > 1$

of the infected compartments approach 0 as a and t increase, which implies that the disease will eventually disappear.

8.2 The PrEP Intervention Strategies for HIV/AIDS Transmission

In this section, we investigate the impact of PrEP intervention on HIV/AIDS transmission in China. We choose $\psi(a) = 0, 0.1, 0.2$ in model (1), respectively. Figure 13a shows the changing trend of cumulative HIV and AIDS cases with respect to $\phi(a)$. More specifically, the cumulative HIV cases will fall by 1.24×10^5 by 2018 when we take $\phi(a) = 0.1$. These results indicate that PrEP treatment can effectively control the

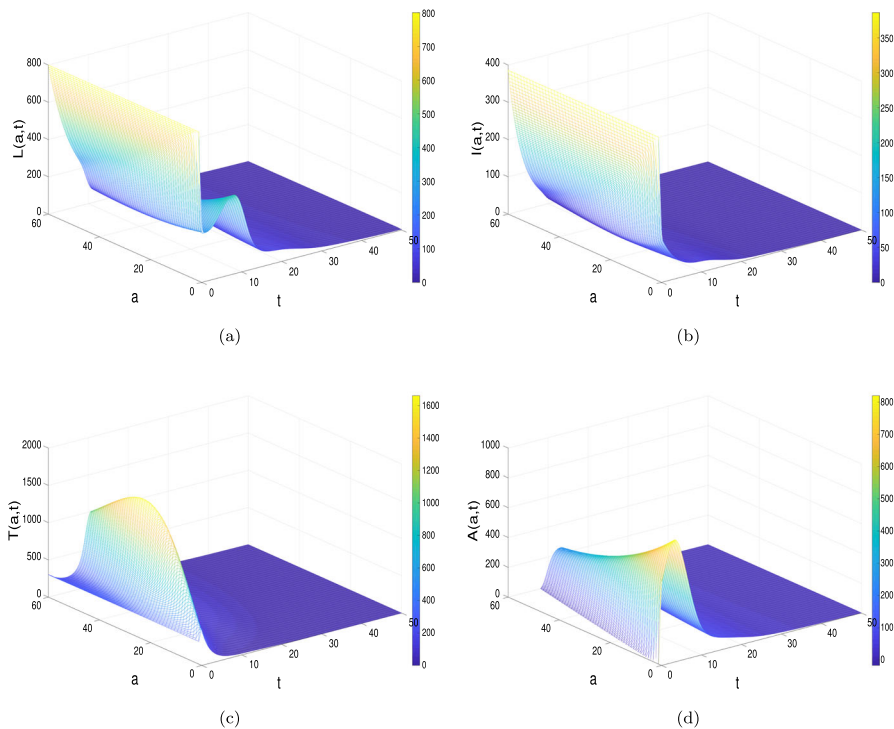


Fig. 12 Dynamical behaviors of the solutions for system (1) when $\mathcal{R}_0 < 1$

transmission of HIV/AIDS. However, when we take $\psi(a) = 0.1$, it means that preventive and control measures need to be taken for all age groups, which will inevitably lead to a waste of medical resources. To implement the cost-effectiveness analysis, we take the following three age-dependent PrEP intervention functions $\psi^*(a), \psi_1^*(a), \psi_2^*(a)$ according to the characteristics of infection rate $\beta(a)$ in Fig. 8f.

$$\psi^*(a) = \begin{cases} 0, & 0 \leq a \leq 15, \\ \frac{1}{250}a, & 15 < a \leq 25, \\ 0.1, & 25 < a \leq 55, \\ -\frac{1}{200}a + \frac{3}{8}, & 55 < a \leq 75, \\ 0, & 75 < a \leq 100, \end{cases}$$

$$\psi_1^*(a) = \begin{cases} 0, & 0 \leq a \leq 15, \\ -\frac{1}{9000}(a - 15)(a - 75), & 15 < a \leq 75, \\ 0, & 75 < a \leq 100, \end{cases} \quad (28)$$

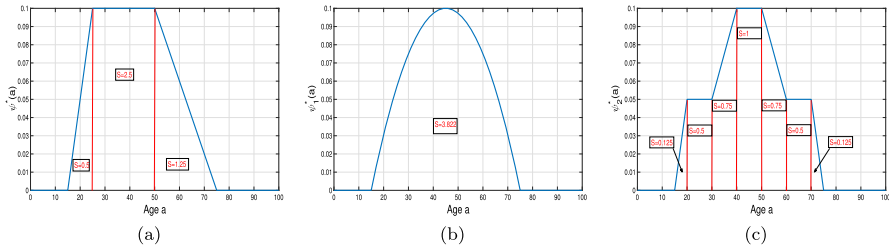


Fig. 13 PrEP cover rate functions

Table 6 Proportion of the population of different age groups to the total population in China, with data from National Bureau of Statistics (2014)

Age group	15–19	20–24	25–29	30–34	35–39	40–44
Proportion	5.16%	5.32%	6.52%	8.81%	7.02%	6.59%
Age group	45–49	50–54	55–59	60–64	65–69	70–74
Proportion	8.10%	8.59%	7.19%	5.21%	5.25%	3.52%

$$\psi_2^*(a) = \begin{cases} 0, & 0 \leq a \leq 15, \\ 0.01(a - 15), & 15 < a \leq 20, \\ 0.05, & 20 < a \leq 30, \\ 0.005a - 0.1, & 30 < a \leq 40, \\ 0.1, & 40 < a \leq 50, \\ 0.35 - 0.005a, & 50 < a \leq 60, \\ 0.05, & 60 < a \leq 70, \\ -0.01(a - 75), & 70 < a \leq 75, \\ 0, & 75 < a \leq 100, \end{cases} \quad (29)$$

and the diagrams of these three functions are shown in Fig. 13a–c, respectively.

In order to investigate the cost-effectiveness of the implementation of PrEP intervention, we introduce two approaches: incremental cost-effectiveness (ICER) and average cost-effectiveness (ACER). The definitions of ACER and ICER from Augusto (2013) are as follows:

$$\begin{aligned} \text{ACER} &= \frac{\text{Total cost incurred on the implementation of PrEP intervention strategy}}{\text{Total cases of HIV infected averted by the intervention strategy}}, \\ \text{ICER} &= \frac{\text{Change in total costs in strategies i and j}}{\text{Change in control benefits in strategies i and j}}. \end{aligned} \quad (30)$$

To calculate the total cost incurred on the implementation of the PrEP intervention strategy in ACER corresponding to $\psi(a)$, $\psi^*(a)$, $\psi_1^*(a)$, $\psi_2^*(a)$, given by (28)–(29), we list the proportion of the population of different age groups to the total population

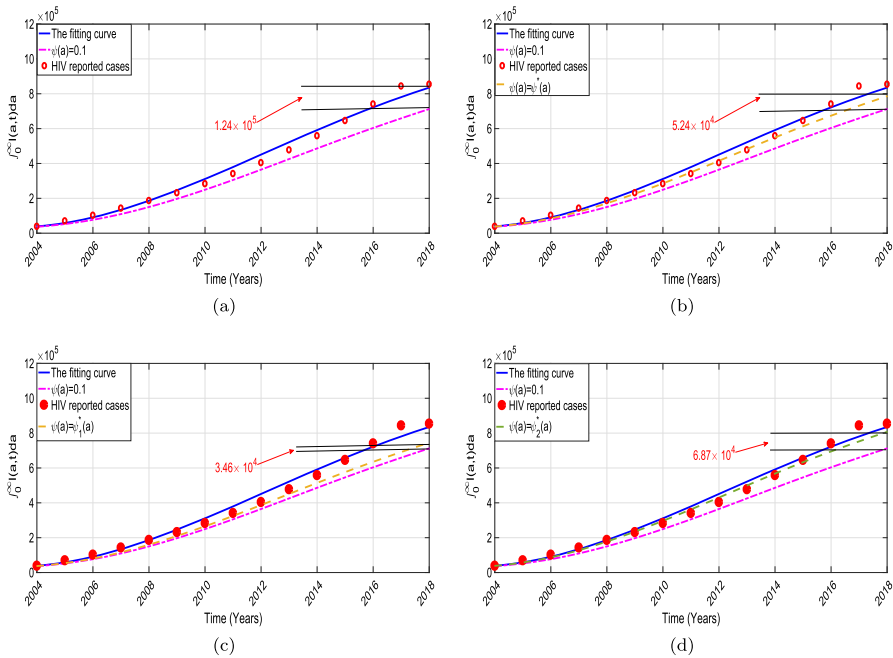


Fig. 14 Impact of different PrEP intervention strategies on HIV/AIDS transmission in China

in Table 6. Based on the data in Wang et al. (2022), we know that the PrEP cost for a single person is 6500 USD per year. Thus, from Fig. 13a, we have the total cost of PrEP with $\psi(a) = 0.1, \mathcal{C}_{\psi^*(a)}$ as follows:

$$\begin{aligned}
 \mathcal{C}_{\psi^*(a)} &= (0.5 \times (5.16\% + 5.32\%) + 2.5 \\
 &\quad \times (6.52\% + 8.81\% + 7.02\% + 6.59\% + 8.1\%) \\
 &\quad + 1.25 \times (8.59\% + 7.19\% + 5.21\% + 5.25\% + 3.52\%)) \\
 &\quad \times 6500N = 8.7646 \times 10^3.
 \end{aligned}
 \tag{31}$$

From Fig. 14b, we can obtain that the total HIV cases averted by the PrEP intervention strategy are 6.32×10^4 . Thus, we have

$$\begin{aligned}
 ACER_{\psi^*(a)} &= \frac{8.7646N}{63.2} \approx 0.13868N, \\
 ICER_{\psi^*(a)} &= \frac{-19822.4N}{-5.68 \times 10^4} \approx 0.34899N,
 \end{aligned}$$

where N represents the total population of China. Similarly, from Figs. 13b–c and 14, we obtain the values of $ACER_{\psi(a)}, ACER_{\psi_1^*(a)}, ACER_{\psi_2^*(a)}, ICER_{\psi_1^*(a)}, ICER_{\psi_2^*(a)}$ which are listed in Table 7.

Applying the ACER cost-effectiveness analysis method, we obtain that intervention $\psi(a) = 0.1$ has the highest ACER value, followed by intervention $\psi(a) = \psi_1^*(a)$,

Table 7 Values of ACER and ICER of $\psi(a) = 0.1$, $\psi^*(a)$, $\psi_1^*(a)$, $\psi_2^*(a)$, which are shown in (28)–(29)

$\psi(a)$	0.1	$\psi^*(a)$	$\psi_1^*(a)$	$\psi_2^*(a)$
ACER	0.23336N	0.13868N	0.218595N	0.06399N
ICER for $\psi(a) = 0.1$	–	0.34899N	0.26814N	0.17434N

intervention $\psi(a) = \psi^*(a)$ and intervention $\psi(a) = \psi_2^*(a)$ as shown in Table 7. Therefore, the cost-effectiveness of the four PrEP intervention strategies, ranging from the most cost-effective to the least cost-effective strategy, is given as intervention $\psi(a) = \psi_2^*(a)$, intervention $\psi(a) = \psi^*(a)$, intervention $\psi(a) = \psi_1^*(a)$, and intervention $\psi(a) = 0.1$. The second row of Table 7 summarizes the calculated ICER values for the intervention strategies. Accordingly, the ICER value of intervention strategy ICER $_{\psi^*(a)}$ is higher than that of PrEP intervention strategies ICER $_{\psi_1^*(a)}$ and ICER $_{\psi_2^*(a)}$. This means that the intervention $\psi(a) = \psi^*(a)$ is more costly and less effective than the intervention $\psi(a) = \psi_1^*(a)$ or intervention $\psi(a) = \psi_2^*(a)$. Thus, intervention $\psi(a) = \psi_1^*(a)$ should be eliminated from the list of intervention strategies. Moreover, based on the numerical simulations about ACER and ICER, we can verify that intervention $\psi(a) = \psi_2^*(a)$ is the most effective intervention strategy of the four strategies.

9 Discussion

In this paper, we formulate a continuous age-structured HIV transmission model to explore the cost-effectiveness of PrEP intervention to eradicate HIV transmission. Previously, we tried to establish a three-age structure model to analyze the prevalence of HIV/AIDS among adolescents (15–24), adults (25–49), and the elderly (≥ 50) (Zhao et al. 2020). However, due to the lack of actual HIV/AIDS data and the limitation of the ordinary differential equations model, we did not study HIV transmission in different age groups in detail. Since HIV transmission is highly sensitive due to higher social activity in certain age groups, in this paper, we tried to identify the age groups to target for effectively slowing down the disease transmission. Our results suggest that we need to take sufficient control strategies for adolescents (15–24) and adults (25–49) in order to prevent further transmission. In addition, we derived the basic reproduction number and showed the existence and stability of the disease-free and endemic steady states of the system in terms of the basic reproduction number. We examined the asymptotic behavior of the coupled system and find that if the basic reproduction number under a PrEP campaign $\mathcal{R}(\psi, \theta) < 1$, then the disease-free equilibrium is stable. If $\mathcal{R}(\psi, \theta) > 1$, the disease persists and the unique endemic equilibrium is stable.

Based on the reported number of HIV/AIDS cases from 2004 to 2018 in China, we estimated the model parameters of the demographic model by using the MCMC method which eventually calculated the basic reproduction number R_0 (1.7955 with 95% CI 1.791–1.802). Moreover, we obtained the probability density function curve

and conducted the sensitivity analysis of R_0 for the demographic model. It is worth mentioning that it is very difficult to use the MCMC method to fit a demographic model. Under the assumption that some age-dependent parameters follow an exponential distribution, we obtained the function form of the age-dependent parameters in the age-structure model from the estimated parameters of the demographic model. In addition, the calculated $\mathcal{R}_0(1.8022)$ of the age-structured model is close to the value of the basic reproduction number R_0 of the demographic model. The above results show that the age-structured model we developed is in line with the actual HIV/AIDS epidemic situations. Finally, to study the cost-effectiveness of PrEP intervention strategies for HIV/AIDS transmission we compared four different strategies where prevention varies with respect to the age class. Stronger interventions are needed to substantially reduce the number of infected individuals and the cost of implementing the strategy. We introduce ICER and ACER approaches to determine the most cost-effective strategy. After calculating ACER and ICER, we claim that the PrEP intervention $\psi(a) = \psi_2^*(a)$ is the most cost-effective intervention strategy among the four strategies. This shows that taking different interventions based on the HIV epidemiological characteristics of different age groups can effectively control the spread of the disease while achieving the lowest cost.

In summary, we have used an age-structured model to explore the effect of PrEP on controlling the spread of HIV and its cost-effectiveness and found that expanding PrEP coverage would be highly effective to prevent disease transmission, but different age-based interventions are necessary to control the disease spread cost-effectively.

Acknowledgements Research of PW is supported by the National Nature Science Foundation of China (No. 12201557), the Foundation of Zhejiang Provincial Education Department (No. Y202249921). Research of HW is partially supported by Natural Sciences and Engineering Research Council of Canada (NSERC) Discovery Grant RGPIN-2020-03911 and NSERC Accelerator Grant RGPAS-2020-00090.

Data availability statement All used data are available on public databases.

Appendix A: The Collection of Real Data

To parameterize the continuous age-structured model for HIV/AIDS transmission in China, we first fit the reported cases from 2004–2018 (Data-Center of China Public Health Science 2021) by the demographic model (25). The numbers of reported HIV/AIDS cases for different age groups from 2004 to 2018 are displayed in Tables 8, 9 and 10.

Table 8 HIV/AIDS reported cases from 2004 to 2008 in China. The data were collected from Data-Center of China Public Health Science (2021)

Year Age	2004		2005		2006		2007		2008	
	HIV	AIDS	HIV	AIDS	HIV	AIDS	HIV	AIDS	HIV	AIDS
15–19	376	17	627	67	771	56	813	110	1043	80
20–24	1690	125	3334	233	4415	301	4407	532	5765	473
25–29	2891	394	5940	775	7118	851	7155	1352	8636	1188
30–34	3119	632	6530	1163	7902	1348	7663	1830	8596	1776
35–39	2167	604	4135	1142	5291	1302	5736	1854	6731	1809
40–44	1269	500	2101	799	2753	1063	2848	1319	3844	1455
45–49	655	263	805	379	963	468	1241	687	1933	870
50–54	430	211	520	401	686	466	804	586	1299	688
55–59	191	107	321	104	448	293	562	447	974	569
60–64	102	65	204	140	328	142	410	366	697	389
65+	72	31	124	71	223	109	339	194	568	285

Table 9 HIV/AIDS reported cases from 2009 to 2013 in China. The data were collected from Data-Center of China Public Health Science (2021)

Year Age	2009		2010		2011		2012		2013	
	HIV	AIDS	HIV	AIDS	HIV	AIDS	HIV	AIDS	HIV	AIDS
15–19	1094	105	1331	156	1545	225	1940	628	2286	581
20–24	6203	589	6795	888	7256	1143	8077	3211	8902	3274
25–29	8403	1361	8275	1796	8861	2048	9564	5431	10,275	5066
30–34	8285	2075	7452	2213	7813	2595	8435	5982	8578	5635
35–39	6870	2330	6586	2546	7128	3120	7440	6059	7382	5638
40–44	4421	1946	4550	2205	5273	2799	6120	5188	6542	5419
45–49	2502	1284	2733	1657	3742	2253	4389	4072	5013	4308
50–54	1484	921	1721	1136	2154	1382	2584	2469	3141	2837
55–59	1335	852	1687	1147	2340	1553	2835	2730	3275	2948
60–64	1044	650	1371	792	1978	1202	2247	2260	2761	2478
65+	1852	950	2423	1272	3945	1941	4101	3436	4645	3743

Table 10 HIV/AIDS reported cases from 2014 to 2018 in China. The data were collected from Data-Center of China Public Health Science (2021)

Year	2014		2015		2016		2017		2018	
	HIV	AIDS	HIV	AIDS	HIV	AIDS	HIV	AIDS	HIV	AIDS
15–19	2972	718	3377	539	3279	581	3283	566	3299	567
20–24	10,597	3383	11,345	2874	11,051	3065	10,758	2870	10,652	3041
25–29	12,135	5524	13,579	5679	13,655	6069	13,390	5807	13,321	5840
30–34	9485	5538	9698	5906	10,287	6193	10,545	6229	11,089	6720
35–39	7905	5627	8201	5851	8232	6085	8919	6036	9279	6818
40–44	7414	5570	8000	6633	8593	6909	9196	6731	9267	7056
45–49	3803	3186	4100	3508	4410	3605	5142	3886	6462	4816
50–54	3342	2881	4008	3508	4996	4037	5900	4590	7138	5422
55–59	2416	1968	2872	2470	3525	2922	4392	3372	5926	4237
60–64	1666	1270	2051	1648	2387	1755	2938	2186	3693	2676
65+	5589	4150	6741	5378	8203	6127	10,249	7431	13,250	9283

Appendix B: Collection of Fitted Curves

The fitted curves of new and cumulative HIV/AIDS cases for different age groups are presented in Figs. 15, 16, 17 and 18.

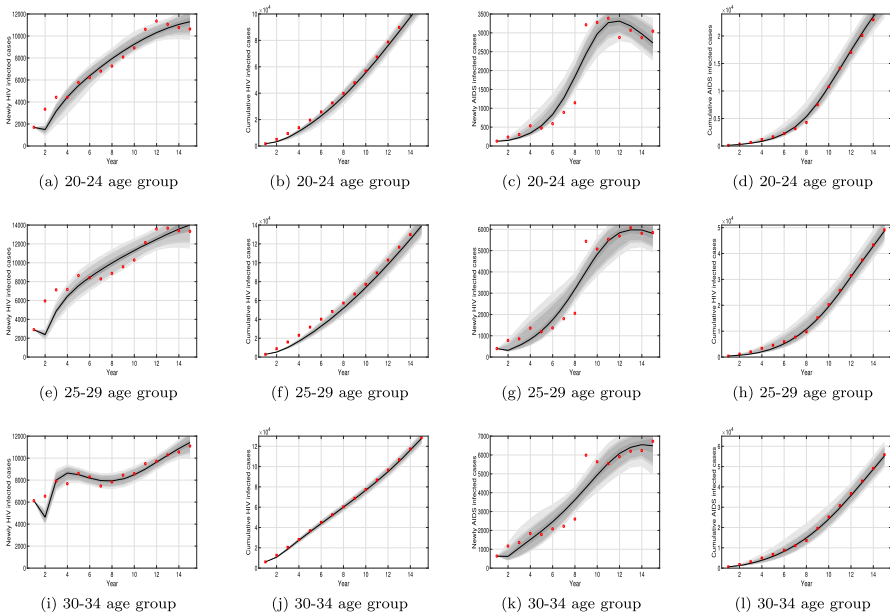


Fig. 15 Fitting curves of the new and cumulative HIV and AIDS reported cases from 2004 to 2018

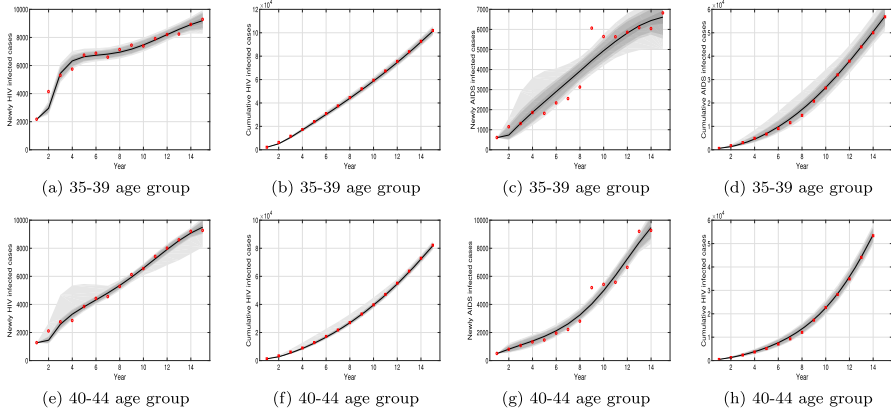


Fig. 16 Fitting curves of the new and cumulative HIV and AIDS reported cases from 2004 to 2018

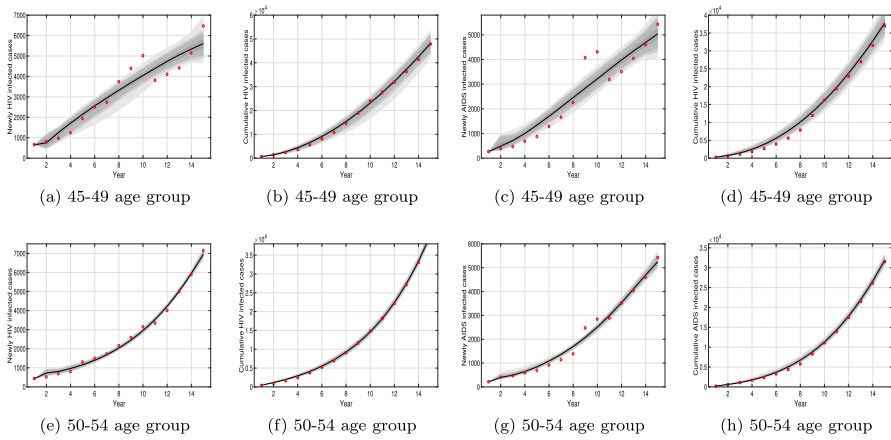


Fig. 17 Fitting curves of the new and cumulative HIV and AIDS reported cases from 2004 to 2018

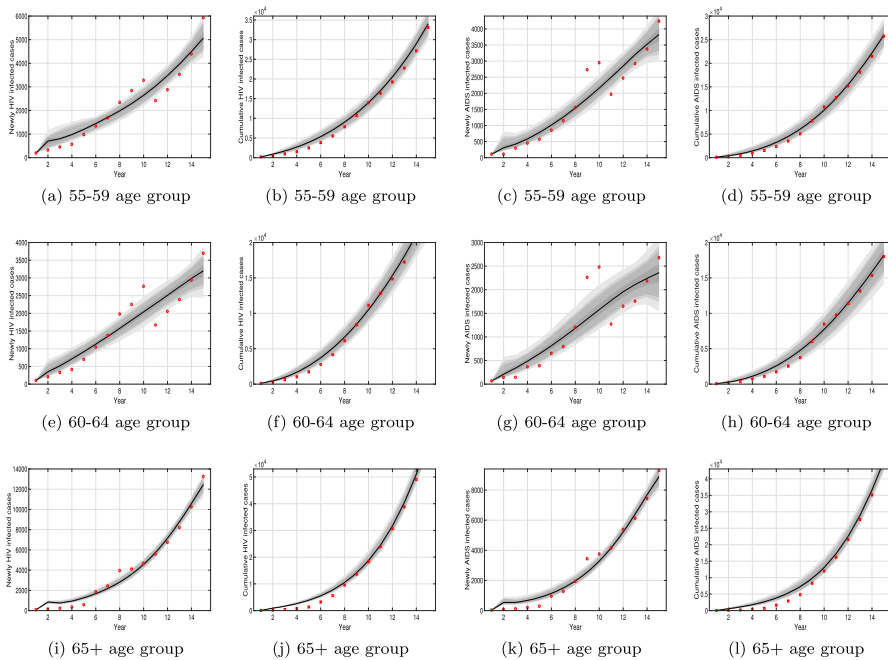


Fig. 18 Fitting curves of the new and cumulative HIV and AIDS reported cases from 2004 to 2018

References

- Agusto F (2013) Optimal isolation control strategies and cost-effectiveness analysis of a two-strain avian influenza model. *Biosystems* 113:155–64
- Angulo O, Lopez-Marcos JC, Milner FA (2007) The application of an age-structured model with unbounded mortality to demography. *Math Biosci* 208:495–520
- Angulo O, Lopez-Marcos JC et al (2010) A numerical method for nonlinear age-structured population models with finite maximum age. *J Math Anal Appl* 361:150–160
- Breda D, Falorian F, Ripoll J, Vermiglio R (2021) Efficient numerical computation of the basic reproduction number for structured populations. *J Comput Appl Math* 384:113165
- Chang K, Zhang Q (2022) Numerical approximation of basic reproduction number for an age-structured HIV infection model with both virus-to-cell and cell-to-cell transmissions. *Math Methods Appl Sci* 44:12851–12859
- Chavez CC, Feng Z (1998) Global stability of an age-structure model for TB and its applications to optimal vaccination strategies. *Math Biosci* 151:135–154
- Data-Center of China Public Health Science (2021) Data directory. <https://www.phsciencedata.cn/Share/en/index.jsp>. Accessed 15 Mar 2021
- Feng Z, Huang W, Chavez CC (2005) Global behavior of a multi-group SIS epidemic model with age structure. *J Differ Equ* 218:292–324
- Feng Z, Feng Y, Glasser JW (2020) Influence of demographically-realistic mortality schedules on vaccination strategies in age-structured models. *Theor Popul Biol* 132:24–32
- Gang H, Liu X, Takeuchi Y (2012) Lyapunov functions and global stability for age-structured HIV infection model. *SIAM J Appl Math* 72:25–38
- Gao D, Munganga MW, Van Den Driessche P, Zhang L (2022) Effects of asymptomatic infections on the spatial spread of infectious diseases. *SIAM J Appl Math* 82:899–923
- Guo T, Qiu Z, Kitagawa K, Iwami S, Rong L (2021) Modeling HIV multiple infection. *J Theor Biol* 509:110502

- Hethcote HW (2000) The mathematics of infectious diseases. *SIAM Rev* 42:599–653
- Kuniya T (2017) Numerical approximation of the basic reproduction number for a class of age-structured epidemic models. *Appl Math Lett* 73:106–112
- Li X, Yang J, Martcheva M (2020) Age structured epidemic modeling. Springer, Cham
- Manoj K, Abbas S (2022) Global dynamics of an age-structured model for HIV viral dynamics with latently infected T cells. *Math Comput Simul* 198:237–252
- Martcheva M, Crispino-O’Connell G (2003) The transmission of meningococcal infection: a mathematical study. *J Math Anal Appl* 283:251–275
- National Bureau of Statistics (2014) China Population and employment statistics yearbook 2014. <http://www.stats.gov.cn/>
- National Bureau of Statistics (2021) China statistical yearbook. <http://www.stats.gov.cn/tjsj/ndsj/2020/indexch.htm>. Accessed 18 Jan 2021
- Nelson PW, Gilchrist MA, Coombs D, Hyman JM, Perelson AS (2004) An age-structured model of HIV infection that allows for variations in the production rate of viral particles and the death rate of productively infected cells. *Math Biosci Eng* 2:267–288
- Qiao Y, Xu Y et al (2019) Epidemiological analyses of regional and age differences of HIV/AIDS prevalence in China, 2004–2016. *Int J Infect Dis* 81:215–220
- Qiu Z, Feng Z (2010) Transmission dynamics of an influenza model with age of infection and antiviral treatment. *J Dyn Differ Equ* 22:823–851
- Rong L, Feng Z, Perelson AS (2007) Mathematical analysis of age-structured HIV-1 dynamics with combination antiretroviral therapy. *SIAM J Appl Math* 67:731–756
- Stavros B, Chavez CC (1991) A general solution of the problem of mixing of subpopulations and its application to risk-and age-structured epidemic models for the spread of AIDS. *Math Med Biol A J IMA* 8(1):1–29
- Sweeting MJ, Angelis D et al (2010) Estimating the distribution of the window period for recent HIV infections: a comparison of statistical methods. *Stat Med* 29:3194–3202
- Wang X, Lou Y, Song X (2017) Age-structured within-host HIV dynamics with multiple target cells. *Stud Appl Math* 138:43–76
- Wang L, Din A, Wu P (2022) Dynamics and optimal control of a spatial diffusion HIV/AIDS model with antiretroviral therapy and pre-exposure prophylaxis treatments. *Math Methods Appl Sci* 45:10136–10161
- Webb GF (2008) Population models structured by age, size, and spatial position. In: Magal P, Ruan S (eds) Structured population models in biology and epidemiology, vol 1936. Lecture notes in mathematics. Springer, New York, pp 1–49
- Wu Z, Wang Y, Detels R, Bulterys M, McGoogan JM (2020a) HIV/AIDS in China. Springer, Singapore
- Wu Z, Wang Y, Detels R, Bulterys M, McGoogan JM (2020b) HIV/AIDS in China: epidemiology, prevention and treatment. Springer, Singapore
- Xue L, Jing S, Wang H (2022) Evaluating strategies for tuberculosis to achieve the goals of WHO in China: a seasonal age-structured model study. *Bull Math Biol* 84:1–50
- Zhang Y, Cai C et al (2020) Disproportionate increase of new diagnosis of HIV/AIDS infection by sex and age-China, 2007–2018. *China CDC Wkly* 5:69–74
- Zhao H, Wu P, Ruan S (2020) Dynamic analysis and optimal control of a three-age-class HIV/AIDS epidemic model in China. *Discrete Contin Dyn Syst Ser B* 25:3491–3521
- Zheng T, Luo Y, Zhou X, Zhang L, Teng Z (2021) Spatial dynamic analysis for COVID-19 epidemic model with diffusion and Beddington–Dengelis type incidence. *Commun Pure Appl Anal*. <https://doi.org/10.3934/cpaa.2021154>

Publisher’s Note Springer Nature remains neutral with regard to jurisdictional claims in published maps and institutional affiliations.

Springer Nature or its licensor (e.g. a society or other partner) holds exclusive rights to this article under a publishing agreement with the author(s) or other rightsholder(s); author self-archiving of the accepted manuscript version of this article is solely governed by the terms of such publishing agreement and applicable law.